Nonconventional glucagon and GLP-1 receptor agonist and antagonist interplay at the GLP-1 receptor revealed in high-throughput FRET assays for cAMP

Oleg G. Chepurny[‡1], ⊙ Minos-Timotheos Matsoukas[§1], George Liapakis[¶], Colin A. Leech[‖], Brandon T. Milliken[**], Robert P. Doyle[‡**2], and George G. Holz[‡ ‡‡3]

From the Departments of ‡Medicine, ‖Surgery, and ‡‡Pharmacology, State University of New York (SUNY), Upstate Medical University, Syracuse, New York 13210, the §Department of Pharmacy, University of Patras, 26500 Patras, Greece, the ¶Department of Pharmacology, School of Medicine, University of Crete, 71003 Heraklion, Crete, Greece, and the **Department of Chemistry, Syracuse University, Syracuse, New York 13244

Edited by Jeffrey E. Pessin

G protein–coupled receptors (GPCRs) for glucagon (GluR) and glucagon-like peptide-1 (GLP-1R) are normally considered to be highly selective for glucagon and GLP-1, respectively. However, glucagon secreted from pancreatic α-cells may accumulate at high concentrations to exert promiscuous effects at the β-cell GLP-1R, as may occur in the volume-restricted microenvironment of the islets of Langerhans. Furthermore, systemic administration of GluR or GLP-1R agonists and antagonists at high doses may lead to off-target effects at other receptors. Here, we used molecular modeling to evaluate data derived from FRET assays that detect cAMP as a read-out for GluR and GLP-1R activation. This analysis established that glucagon is a nonconventional GLP-1R agonist, an effect inhibited by the GLP-1R orthosteric antagonist exendin(9–39) (Ex(9–39)). The GluR allosteric inhibitors LY2409021 and MK 0893 antagonized glucagon and GLP-1 action at the GLP-1R, whereas des-His[1]-[Glu[9]]glucagon antagonized glucagon action at the GluR, while having minimal inhibitory action versus glucagon or GLP-1 at the GLP-1R. When testing Ex(9–39) in combination with des-His[1]-[Glu[9]]glucagon in INS-1 832/13 cells, we validated a dual agonist action of glucagon at the GluR and GLP-1R. Hybrid peptide GGP817 containing glucagon fused to a fragment of peptide YY (PYY) acted as a triagonist at the GluR, GLP-1R, and neuropeptide Y2 receptor (NPY2R). Collectively, these findings provide a new triagonist strategy with which to target the GluR, GLP-1R, and NPY2R. They also provide an impetus to reevaluate prior studies in which GluR and GLP-1R agonists and antagonists were assumed not to exert promiscuous actions at other GPCRs.

New approaches to the treatment of type 2 diabetes (T2D)[4] and obesity focus on the design of synthetic peptides that act as dual agonists or triagonists at GTP-binding protein-coupled receptors (GPCRs) and that incorporate amino acid motifs of the hormones glucagon, glucagon-like peptide-1 (GLP-1), glucose-dependent insulinotropic hormone (GIP), and PYY (1–6). These hybrid synthetic peptides are under investigation because of their predicted beneficial effects to control energy expenditure, appetite, and systemic glucose homeostasis (7–9). Glucagon, GLP-1, and GIP bind family B GPCRs corresponding to the glucagon receptor (GluR), GLP-1 receptor (GLP-1R), and GIP receptor (GIP-R) (10), whereas the family A neuropeptide Y2 receptor (NPY2R) recognizes PYY in the forms of PYY(1–36) and PYY(3–36) (11).

The GluR, GLP-1R, and GIP-R are expressed on multiple cell types, including hepatocytes (GluR), adipocytes (GluR and GIP-R) (8, 12), and pancreatic β-cells of the islets of Langerhans (GLP-1R and GIP-R) (13, 14). Glucagon and GIP exert catabolic actions to stimulate energy expenditure through glycogenolysis and lipolysis, whereas GLP-1 and GIP simulate insulin secretion so that levels of blood glucose are reduced. Whereas glucagon is secreted from islet α-cells, GLP-1 and GIP are primarily secreted from enteroendocrine L-cells (GLP-1) and K-cells (GIP) that line the wall of the intestinal tract. Interestingly, L-cells co-secrete GLP-1 and PYY in response to nutrients present within the intestinal lumen (15). The PYY(1–36) precursor that is released is processed by dipeptidyl peptidase-4 (DPP-4) to generate circulating PYY(3–36) that crosses the blood–brain barrier so that it may suppress appetite by binding to NPY2R located on hypothalamic neurons (16, 17). GLP-1 is also present within the nucleus solitarius of the brainstem (18), and it, too, participates in the suppression of appetite by binding to a diffuse network of GLP-1 receptors located within the central nervous system (19).

ASBMB

To optimize dual agonist or triagonist peptides for therapeutic purposes, it is necessary to achieve "balanced agonism" in which simultaneous stimulation of multiple GPCRs is achieved across the desired concentration range. It is also necessary to identify the selectivity with which such peptides activate GPCRs, and in this regard it is necessary to identify potential nonconventional actions that allow them to exert off-target effects. Furthermore, the optimization of dual or triagonists requires detailed knowledge of their molecular mechanisms of action. In this regard, modeling of GPCR structure/conformation is facilitated by the availability of GPCR agonists and antagonists that aid in the identification of orthosteric and allosteric mechanisms of ligand binding and receptor activation. One such agonist for the GLP-1R is exendin-4 (Ex-4) (20, 21). Four antagonists of family B GPCRs are exendin-(9–39) (Ex(9–39)) acting at an orthosteric site on the GLP-1R (20–22), des-His[1]-[Glu[9]]glucagon acting at an orthosteric site on the GluR (23), and LY2409021 (24) and MK 0893 (25) acting at an allosteric site on the GluR (26).

Recently, we developed a microplate high-throughput fluorescence resonance energy transfer (FRET) assay that monitors the kinetics with which GPCR agonists stimulate an increase or decrease in levels of the second messenger adenosine-3′,5′-cyclic monophosphate (cAMP) in cell monolayers (27). This assay uses the H188 biosensor designed by Klarenbeek *et al.* (28) in which cAMP binds directly to a modified Epac1 protein that is flanked by mTurquoise2Δ FRET donor and tandem cp173 Venus–Venus FRET acceptor chromophores. Here, we used this FRET assay to discover nonconventional actions of family B GPCR agonists and antagonists, while also investigating the pharmacological properties of a hybrid peptide (GGP817) that incorporates amino acid sequences present within glucagon and PYY. Our analysis reveals unexpected features of GPCR agonist and antagonist action, while also establishing GGP817 to be a prototype triagonist at the GluR, GLP-1R, and NPY2R.

Results

FRET-based assays for GPCR agonist and antagonist action

FRET assays were performed in a 96-well format so that it was possible to monitor the kinetics and dose dependence with which GPCR agonists stimulated or inhibited cAMP production. For this purpose, we used HEK293 cells that stably express recombinant GPCRs and that were virally transduced with H188, thereby allowing FRET to be monitored in real time using confluent cell monolayers. This approach was complemented by our use of a new clone of HEK293-H188-C24 cells that stably express H188 (27) and that were transiently transfected with select recombinant GPCRs. The GPCR agonists tested included the NPY2R agonist PYY(3–36) that inhibits cAMP production or the GPCR agonists GLP-1, exendin-4, glucagon, and GIP that stimulate cAMP production (Fig. 1). Also tested were GPCR antagonists previously reported to be selective for the GluR (des-His[1]-[Glu[9]]glucagon, LY2409021, and MK 0893) or the GLP-1R (exendin(9–39)) or NPY2R (BIIE0246) (Fig. 1) (29). Finally, we tested for novel dual or triagonist properties of GGP817, a synthetic hybrid peptide that contains full-length glucagon to which a 12-amino acid

C-terminal fragment of PYY is fused at the C terminus of glucagon (Fig. 1). Importantly, control experiments verified that GLP-1, exendin-4, glucagon, and GGP817 failed to alter levels of cAMP in HEK293 cells that expressed H188 but that were not transfected with recombinant GPCRs (Fig. S1, *a–f*).

Glucagon and LY2409021 both target glucagon and GLP-1 receptors

Using HEK293 cells that stably express the rat glucagon receptor (HEK293-GluR), and that were virally transduced with H188, it was confirmed that glucagon acts as a GluR agonist to raise levels of cAMP in a dose-dependent manner (Fig. 2, a_1–a_3) (30). LY2409021 dose-dependently blocked this action of glucagon (Fig. 2, b_1–b_3), but it exerted no effect when tested alone (Fig. S2*a*).

EC_{50} and IC_{50} values for glucagon agonist or LY2409021 antagonist action at the rat GluR were 400 pM and 1.8 μM, respectively (Fig. 2, a_3 and b_3). Consistent with a prior report concerning glucagon action at the GLP-1R (5), high concentrations of glucagon (1–100 nM) raised levels of cAMP in HEK293-GLP-1R cells expressing the human GLP-1R (Fig. 2, c_1–c_3). This action of glucagon was also blocked by LY2409021 (Fig. 2, d_1–d_3), whereas LY2409021 exerted no effect alone at the GLP-1 R (Fig. S2*b*). EC_{50} and IC_{50} values for glucagon agonist and LY2409021 antagonist actions at the GLP-1R were 4.9 nM and 1.2 μM, respectively (Fig. 2, c_3 and d_3). LY2409021 antagonism of glucagon action at the GLP-1R was also measured using HEK293-H188 C24 cells transiently transfected with the human GLP-1R (Fig. S3, *a–d*). Although glucagon acted with lower potency than GLP-1 at the GLP-1R, it exhibited full agonist properties because 100 nM glucagon stimulated a 60% maximal change of the H188 FRET ratio (ΔFRET) when it was tested at either the GluR or the GLP-1R (*cf.* Fig. 2, a_1 and c_1).

LY2409021 blocks GLP-1 and Ex-4 agonist action at the GLP-1R

As expected on the basis of prior studies (31), low concentrations of GLP-1 raised levels of cAMP in HEK293-GLP-1R cells (Fig. 3, a_1–a_3). Unexpectedly, this action of GLP-1 (100 pM) was blocked by LY2409021 (Fig. 3, b_1–b_3). Similarly, Ex-4 acted as an agonist at the GLP-1R (Fig. 3, c_1–c_3), and this action of Ex-4 (100 pM) was blocked by LY2409021 (Fig. 3, d_1–d_3). EC_{50} values for GLP-1 and Ex-4 agonist action at the GLP-1R were 65 and 30 pM, respectively (Fig. 3, a_3 and c_3). IC_{50} values for LY2409021 to block agonist actions of GLP-1 and Ex-4 at the GLP-1R were 7 and 12 μM, respectively (Fig. 3, b_3 and d_3). Thus, when comparing the antagonist action of LY2409021 to block GLP-1 agonist action at the GLP-1R (Fig. 3b_3), or glucagon agonist action at the GluR (Fig. 2b_3), or glucagon action at the GLP-1R (Fig. 2d_3), the rank order of IC_{50} values was 7, 1.8, and 1.2 μM, respectively.

LY2409021 is a GIP-R antagonist but fails to block adenosine action at A2$_B$ receptors

LY2409021 consistently blocked peptide hormone agonist actions at all family B GPCRs tested. This was the case not only for the GluR and GLP-1R, but also for the GIP-R when testing the action of GIP using HEK293-GIP-R cells that stably express

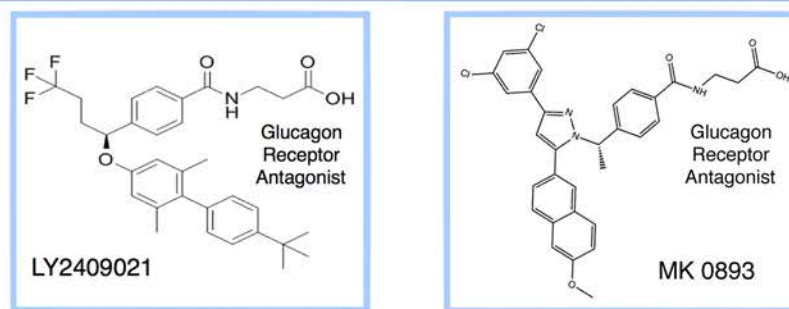| Peptide	Sequence	AA
PYY(3-36)	IKPEAPGEDASPEELNRYYASLRHYLNLVTRQRY-NH2	34
GGP817	HSQGTFTSDYSKYLDSRRAQDFVQWLMNTRHYLNLVTRQRY-NH2	41
Glucagon	HSQGTFTSDYSKYLDSRRAQDFVQWLMNT	29
des-His¹-[Glu⁹]-Glucagon	SQGTFTSEYSKYLDSRRAQDFVQWLMNT-NH2	28
GLP-1	HAEGTFTSDVSSYLEGQAAKEFIAWLVKG-NH2	30
Ex-4	HGEGTFTSDLSKQMEEEAVRLFIEWLKNGGPSSGAPPPS-NH2	39
Ex(9-39)	DLSKQMEEEAVRLFIEWLKNGGPSSGAPPPS-NH2	31
GIP	YAEGTFISDYSIAMDKIHQQDFVNWLLAQKGKKNDWKHNITQ	42

Figure 1. Peptide sequence alignments and GluR antagonist structures. *Top panel,* color-coding of synthetic peptides where conserved amino acid residues labeled in *blue* are present in PYY(3–36) and the C terminus of GGP817. Amino acids labeled in *red* are present in glucagon, des-His¹-[Glu⁹]glucagon, the N terminus of GGP817, GLP-1, Ex-4, Ex(9–39), and GIP. *AA* indicates amino acid chain length. *Bottom panels,* structures of the glucagon receptor antagonists LY2409021 and MK 0893.

the rat GIP-R (Fig. S4, *a–c*) (32). However, LY2409021 failed to block cAMP-elevating actions of adenosine that are mediated by its $A2_B$ receptor that is a family A GPCR and that is an endogenous GPCR expressed in parental HEK293 cells (Fig. S5, *a* and *b*) (33). Instead, this action of adenosine was blocked by the $A2_B$ receptor antagonist GS 6201 (Fig. S5, *c* and *d*). Thus, LY2409021 exhibited high selectivity for family B GPCRs, as expected if it acts as an allosteric inhibitor in which it specifically interacts with a conserved binding motif within the GluR, GLP-1R, and GIP-R (see below; Fig. 6).

LY2409021 blocks GGP817 agonist action at the GluR and GLP-1R

Here, we designed the synthetic hybrid peptide GGP817 with the expectation that it might act as a triagonist because it incorporates amino acid residues found within glucagon, GLP-1, and PYY. For example, because glucagon is an agonist at the GluR, and also an agonist at the GLP-1R, GGP817 might possess triagonist properties in which it activates the GluR and GLP-1R in addition to NPY2R. When tested using HEK293-GluR cells, GGP817 exhibited agonist action at the GluR (Fig. 4, a_1–a_3), and this effect was blocked by LY2409021 (Fig. 4, b_1–b_3). However, GGP817 also exhibited agonist action at the GLP-1R in HEK293-GLP-1R cells (Fig. 4, c_1–c_3), and this effect was

blocked by LY2409021 (Fig. 4, d_1–d_3). Note that when it was tested using these GluR- and GLP-1R– expressing HEK293 cells, GGP817 was less potent compared with the naturally occurring receptor ligands glucagon and GLP-1. Also note that GGP817 failed to exhibit agonist action at the GIP-R (Fig. S4d).

The EC_{50} value for GGP817 agonist action at the GluR was 183 nM (Fig. $4a_3$), and it was 61 nM for the GLP-1R (Fig. $4c_3$). Still, when GGP817 was tested at a saturating concentration (3,000 nM), it acted as a full agonist at both the GluR and the GLP-1R. This was established by monitoring its ability to stimulate a 60% maximal ΔFRET in the cAMP assay. Of interest, the antagonist potency of LY2409021 at the GluR and GLP-1R in assays using GGP817 resembled that which was observed when testing LY2409021 in assays using glucagon as a stimulus for GluR or GLP-1R activation (*cf.* Figs. 2, b_3 and d_3, and 4, b_3 and d_3). When comparing antagonist actions of LY2409021 to block GGP817 agonist action at the GluR (Fig. $4b_3$) or GGP817 agonist action at the GLP-1R (Fig. $4d_3$), the IC_{50} values were 908 nM and 1.6 μM, respectively.

Antagonist properties of MK 0893 at the GluR and GLP-1R

MK 0893 is a GluR antagonist that is structurally related to LY2409021 (26), and we confirmed that it acted as an antagonist of glucagon agonist action at the GluR in HEK293-
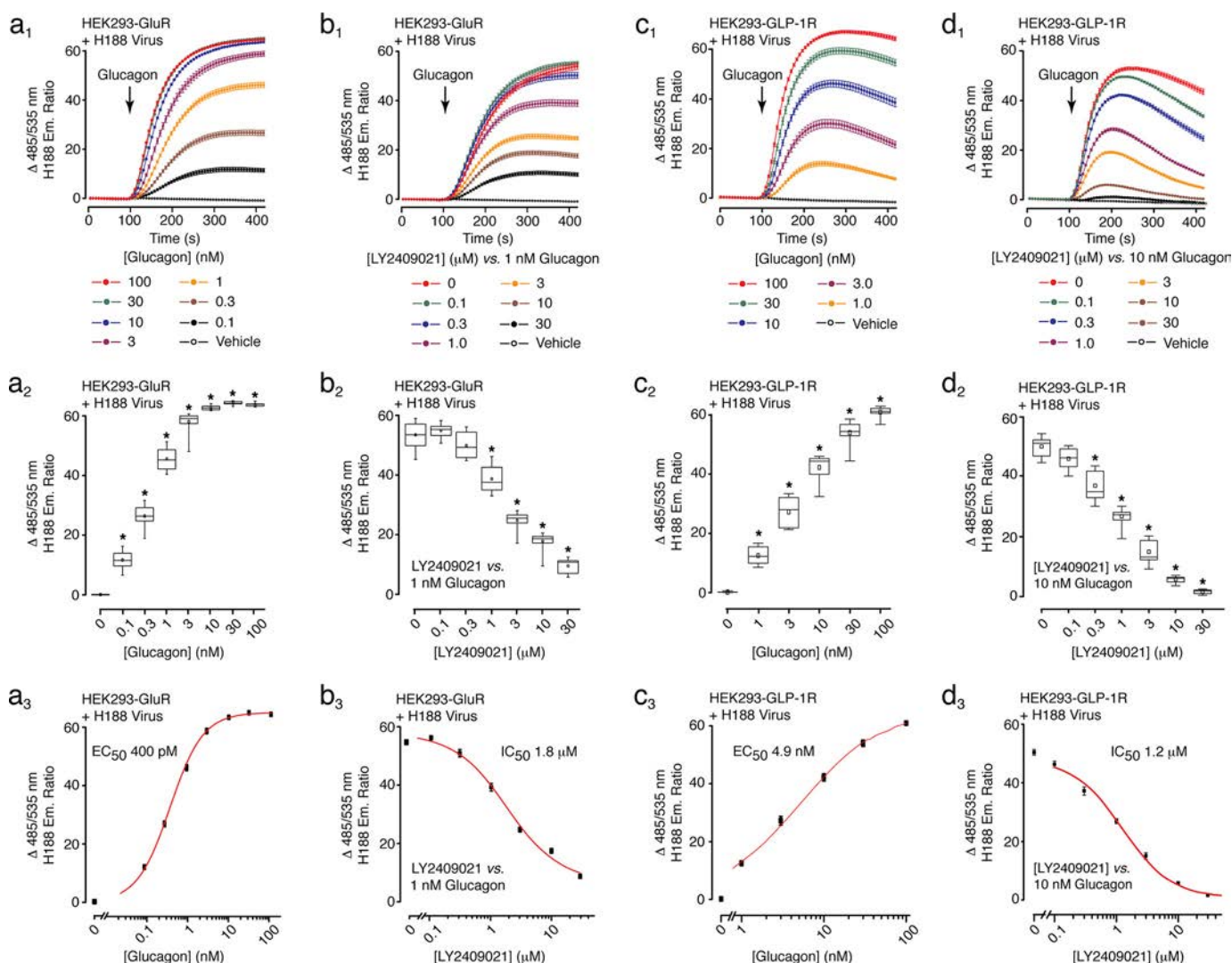
ASBMB

Figure 2. LY2409021 blocks glucagon agonist action at the GluR and GLP-1R. $a_1–a_3$, FRET data (a_1), box-and-whisker plot (a_2), and dose-response plot (a_3) summarizing findings in which glucagon (0.1–100 nM) exerted a dose-dependent action (EC_{50} 400 pM) to increase levels of cAMP in HEK293-GluR cells transduced with H188. $b_1–b_3$, LY2409021(IC_{50} 1.8 μM) blocked glucagon (1 nM) action in HEK293-GluR cells transduced with H188. $c_1–c_3$, glucagon (EC_{50} 4.9 nM) increased levels of cAMP in HEK293-GLP-1R cells transduced with H188. $d_1–d_3$, LY2409021 (IC_{50} 1.2 μM) blocked glucagon (1 nM) action in HEK293-GLP-1R cells transduced with H188. * indicates a p value of < 0.01, one-way ANOVA with post hoc Tukey. Comparisons in a_2 and c_2 are between cells not treated (vehicle control) or treated with the indicated concentrations of glucagon. Comparisons in b_2 and d_2 are between cells treated with glucagon in the absence or the presence of the indicated concentrations of LY2409021. For this figure and all subsequent figures using GPCR antagonists, cells were pretreated with the antagonist for 20 min prior to initiating the assay in which the GPCR agonist was administered in combination with the same concentration of antagonist as was used for the pretreatment.

GluR cells (Fig. S6a). However, for HEK293-GLP-1R cells, the agonist actions of glucagon and GLP-1 were also inhibited by MK 0893 (Fig. S6, *b* and *c*), thereby demonstrating that MK 0893 is not a specific GluR antagonist. Similar to LY2409021, MK 0893 exerted no effect on its own in these GluR- and GLP-1R– expressing HEK293 cell lines (Fig. S6, *d* and *e*). When comparing the actions of LY2409021 and MK 0893, it was also established that both antagonists inhibited the agonist actions of glucagon and GLP-1 in rat INS-1 832/13 insulinoma cells (see below; Fig. 7) that are a model system for studies of pancreatic β-cell function (34) and that co-express endogenous GluR and GLP-1R. Collectively, these findings established the promiscuous nature with which LY2409021 and MK 0893 exerted antagonist effects at family B GPCRs.

Ex(9–39) blocks GLP-1R activation by GLP-1, Ex-4, glucagon, and GGP817

Ex(9–39) exerted its expected antagonist action when testing GLP-1 and Ex-4 in HEK293-GLP-1R cells (Fig. 5, $a_1–a_3$ and $b_1–b_3$) (20, 21). IC_{50} values for Ex(9–39) were 17 and 47 nM when testing GLP-1 or Ex-4, respectively (Fig. 5, a_3 and b_3). However, Ex(9–39) also blocked the actions of glucagon and GGP817 in HEK293-GLP-1R cells (Fig. 5, $c_1–c_3$ and $d_1–d_3$). IC_{50} values for Ex(9–39) were 40 and 42 nM when testing glucagon and GGP817, respectively (Fig. 5, c_3 and d_3).

Although glucagon signaled through the GLP-1R to raise levels of cAMP, the converse was not true when evaluating GLP-1R agonist or antagonist action at the GluR. Thus, GLP-1, Ex-4, and Ex(9–39) alone were without effect when tested in
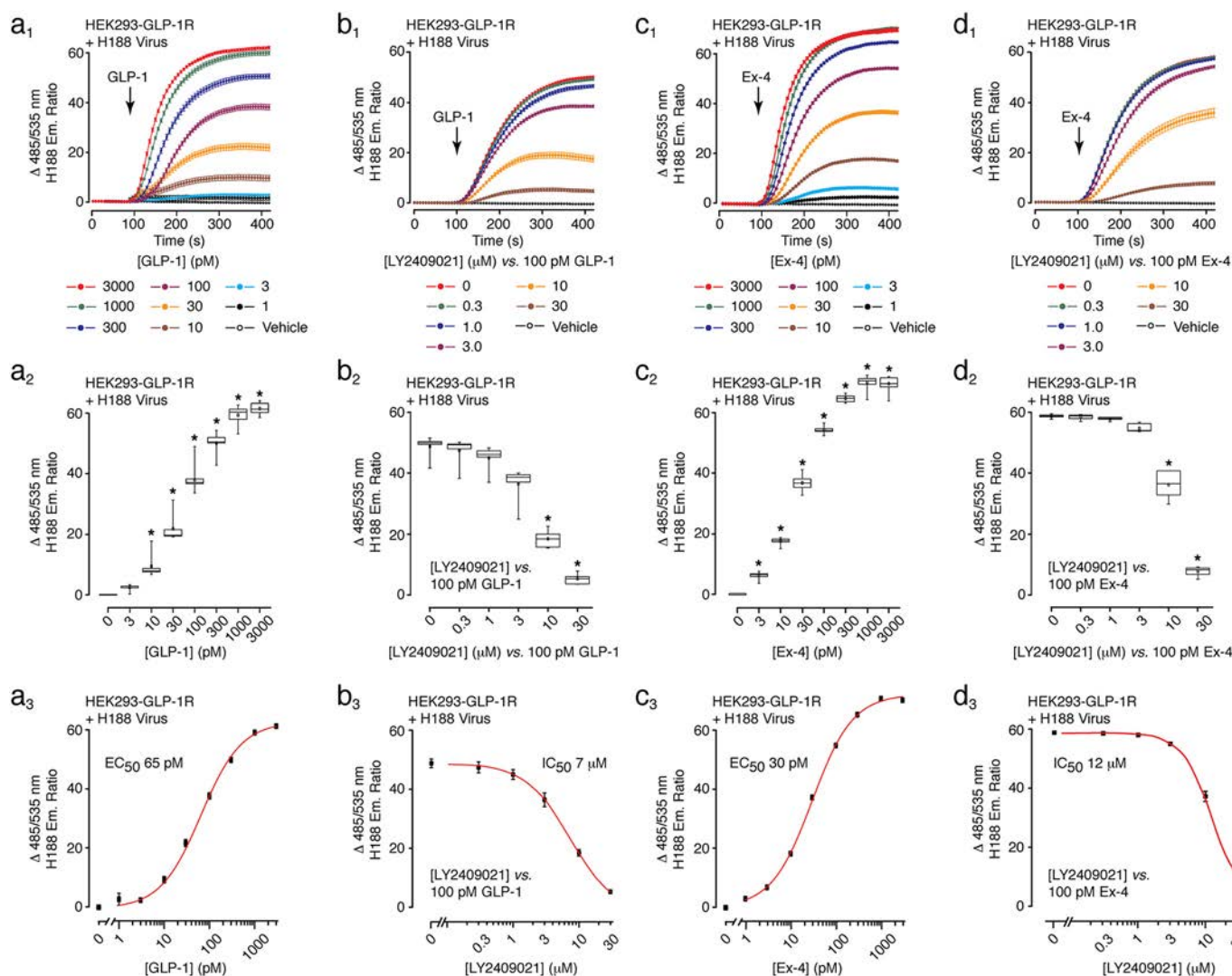
Figure 3. LY2409021 blocks GLP-1 and Ex-4 agonist action at the GLP-1R. a_1–a_3, FRET data (a_1), box-and-whisker plot (a_2), and dose-response plot (a_3) summarizing findings in which GLP-1 (EC_{50} 65 pm) increased levels of cAMP in HEK293-GLP-1R cells transduced with H188. b_1–b_3, LY2409021 (IC_{50} 7 μm) blocked GLP-1 (100 pm) action in HEK293-GLP-1R cells transduced with H188. c_1–c_3, Ex-4 (EC_{50} 30 pm) increased levels of cAMP in HEK293-GLP-1R cells transduced with H188. d_1–d_3, LY2409021(IC_{50} 12 μm) blocked Ex-4 (100 pm) action in HEK293-GLP-1R cells transduced with H188. * indicates a *p* value of < 0.01, one-way ANOVA with post hoc Tukey. Comparisons in a_2 and c_2 are between cells not treated (vehicle control) or treated with the indicated concentrations of GLP-1 or Ex-4. Comparisons in b_2 and d_2 are between cells treated with either GLP-1 or Ex-4 in the absence or the presence of the indicated concentrations of LY2409021.

HEK293-GluR cells (Fig. S7, *a–c*). Because Ex(9–39) failed to antagonize the agonist actions of glucagon and GGP817 at the GluR in HEK293-GluR cells (Fig. 7, *d* and *e*), Ex(9–39) is a specific antagonist of GLP-1R activation and is without significant effect at the GluR.

Computational modeling of LY2409021 binding to the GluR and GLP-1R

Previous structural biology studies used small molecule allosteric inhibitors of the GluR (NNC0640 and MK-0893) (26, 35) or the GLP-1R (NNC0640 and PF-06372222) (36) to identify their binding sites located at the interfaces between transmembrane helices (TMs) 5–7 of these receptors. Using computational receptor modeling, we sought to predict the potential binding site where LY2409021 interacts with the GLP-1R. In this regard, we made use of available data concerning binding of MK 0893 to the GluR (26). Our docking studies using homology

models of family B receptors predict a conserved mode of binding for LY2409021 at the rat GLP-1R and also GluR (Fig. 6, *a–c*). However, it should be noted that future receptor mutagenesis studies would be required to obtain full validation of these predicted interactions.

For both the GLP-1R and GluR, the carboxyl group of LY2409021 is predicted to form a salt bridge with the receptor's R2.47b amino acid residue located in TM2 (Fig. 6, *b* and *c*), as indicated using the Wooten numbering scheme (37). This residue in the GluR is already established to be a significant factor determining direct receptor interactions with downstream G_s proteins (36). The hydrophobic surface of TM5 has several hydrophobic aliphatic residues that are conserved in family B GPCRs and that are likely to interact with the trimethyl group of LY2409021, as inferred from the structure of MK 0893. These are I5.58b, I/V6.52b, L5.65b, and V/L5.61b. The aromatic benzene group of LY2409021 is predicted to form hydrophobic
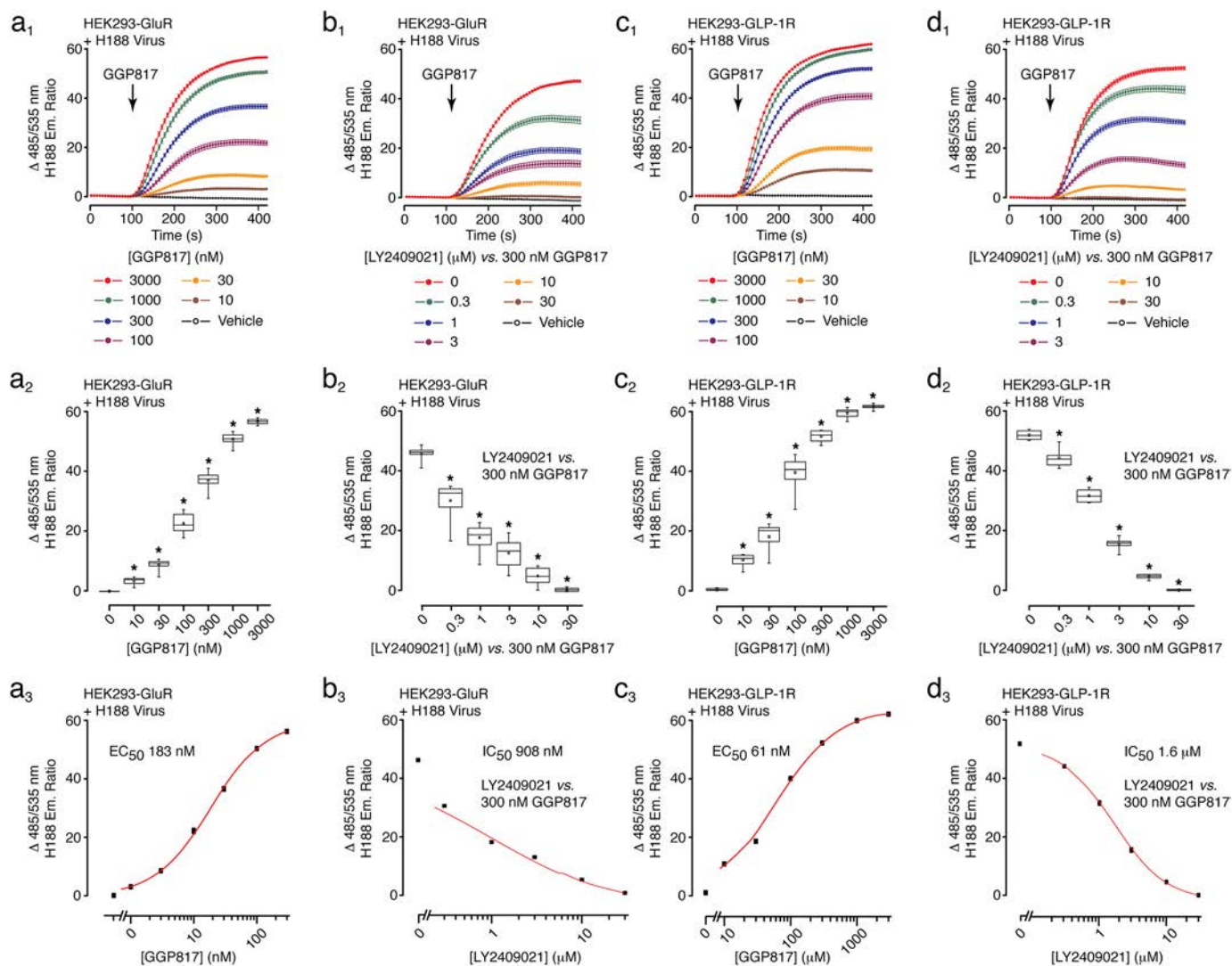
Figure 4. LY2409021 blocks GGP817 agonist action at the GluR and the GLP-1R. a_1–a_3, FRET data (a_1), box-and-whisker plot (a_2), and dose-response plot (a_3) summarizing findings in which GGP817 (EC$_{50}$ 183 nM) increased levels of cAMP in HEK293-GluR cells transduced with H188. b_1–b_3, LY2409021 (IC$_{50}$ 908 nM) blocked GGP817 (300 nM) action in HEK293-GluR cells transduced with H188. c_1–c_3, GGP817 (EC$_{50}$ 61 nM) increased levels of cAMP in HEK293-GLP-1R cells transduced with H188. d_1–d_3, LY2409021 (IC$_{50}$ 1.6 μM) blocked GGP817 (300 nM) action in HEK293-GLP-1R cells transduced with H188. * indicates a p value of <0.01, one-way ANOVA with post hoc Tukey. Comparisons in a_2 and c_2 are between cells not treated (vehicle control) or treated with the indicated concentrations of GGP817. Comparisons in b_2 and d_2 are between cells treated with GGP817 in the absence or the presence of the indicated concentrations of LY2409021.

interactions with L6.43b, present in both the GLP-1R and the GluR. L7.56b is also a crucial contact for the aromatic ring of LY2409021, and it is conserved among family B GPCRs. The two remaining aromatic groups of LY2409021 are predicted to sandwich around the aliphatic chain of K6.40b located in the GLP-1R (Fig. 6b) or R6.40b in the GluR (Fig. 6c). S6.41b forms a hydrogen bond with the only hydrogen donor of LY2409021, and the antagonist's trifluoro group, pointing outwards, probably interacts with the hydrophobic region of the membrane bilayer.

Computational modeling of GLP-1 and glucagon binding to the GLP-1R

Amino acid residues of the human GLP-1R that mediate binding of GLP-1 were previously identified by crystallography and cryo-EM (38, 39). Furthermore, the detailed nature of glucagon binding to the extracellular domain (ECD) of the GluR

was established by determination of the crystal structure of the GluR in complex with a glucagon analogue (40). The main recognition interface for GLP-1 within the ECD of the GLP-1R is governed by hydrophobic ligand–receptor interactions (Fig. 6d). Mainly, Phe-28, Ile-29, Leu-32, and Val-33 of GLP-1 interact in the receptor's hydrophobic pocket formed by Val-36, Trp-39, Tyr-69, Tyr-88, Leu-89, Pro-90, Trp-91, and Leu-123 (Fig. 6d), all of which are conserved in the rat GLP-1R.

Glucagon, however, possesses Phe-22 and Val-23 (instead of Ile-29) and Leu-6 and Met-27 (instead of Val-33), and our analysis indicates that it binds to the GLP-1R ECD in a manner similar to that of GLP-1 (Fig. 6e). In our ECD computational model for the GLP-1R, Val-23 of glucagon interacts with Tyr-88, Leu-89, Pro-90, and Trp-91, whereas Met-27 penetrates deeper into the hydrophobic pocket to interact with Tyr-69 and Leu-123. Note that Phe-22 and Leu-26 of glucagon form the
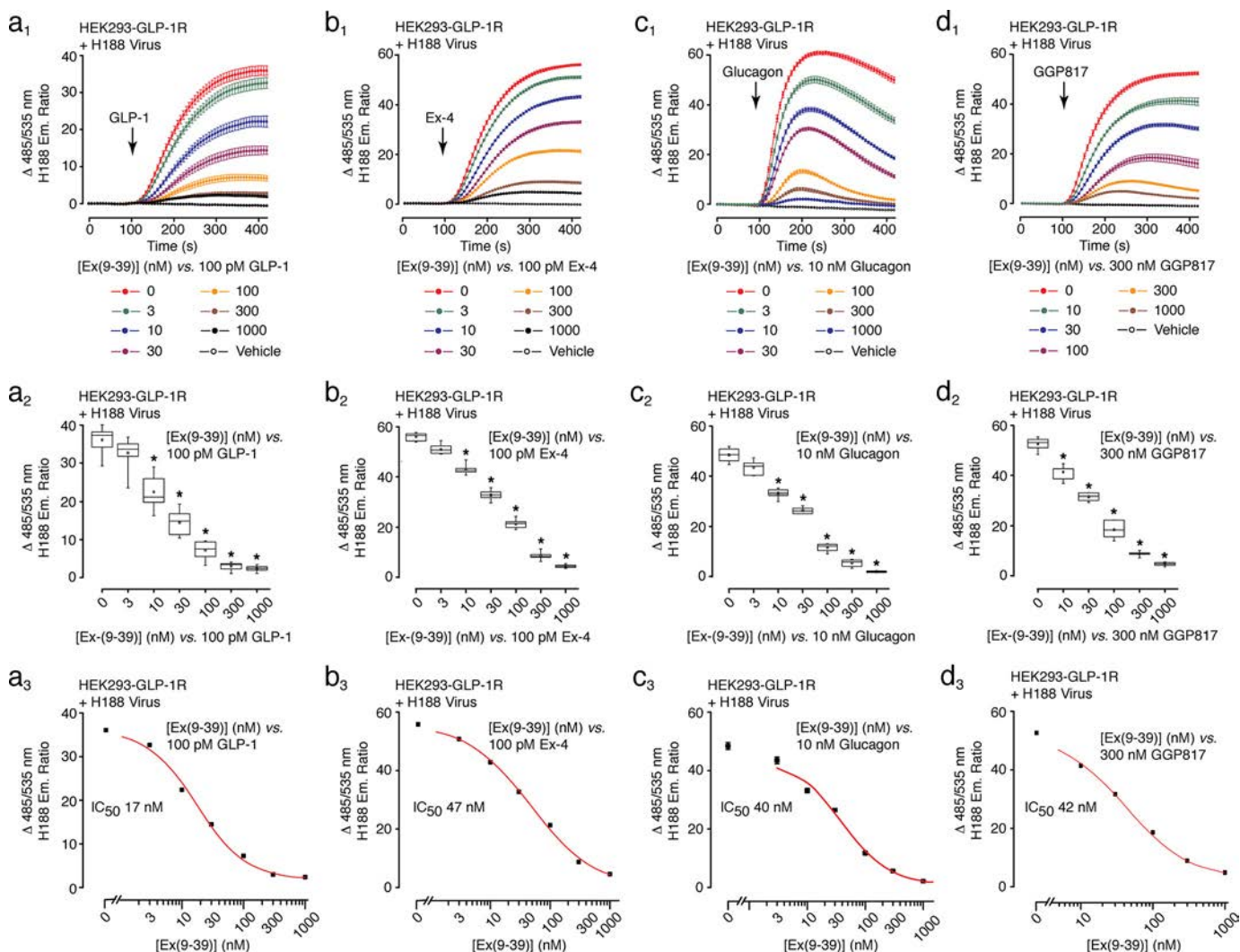
Figure 5. Ex(9–39) blocks GLP-1R activation by GLP-1, Ex-4, glucagon, and GGP817. a_1–a_3, FRET data (a_1), box-and-whisker plot (a_2), and dose-response plot (a_3) summarizing findings in which Ex(9–39) (IC$_{50}$ 17 nM) blocked GLP-1 (100 pM) action in HEK293-GLP-1R cells. b_1–b_3, Ex(9–39) (IC$_{50}$ 47 nM) blocked Ex-4 (100 pM) action in HEK293-GLP-1R cells. c_1–c_3, Ex(9–39) (IC$_{50}$ 40 nM) blocked glucagon (10 nM) action in HEK293-GLP-1R cells. d_1–d_3, Ex(9–39) (IC$_{50}$ 42 nM) blocked GGP817 (300 nM) action in HEK293-GLP-1R cells. * indicates a *p* value of < 0.01, one-way ANOVA with post hoc Tukey. Comparisons in a_2–d_2 are between cells not treated (vehicle control) or treated with the indicated concentrations of Ex(9–39).

same interactions as Phe-28 and Leu-2 of GLP-1 (*cf.* Fig. 6, *d* and *e*) (38). Our GLP-1R ECD model is consistent with the report that Phe-22, Val-23, Leu-26, and Met-27 of glucagon, when mutated to alanine, severely disrupt glucagon binding to the GluR (41).

Computational modeling of Ex(9–39) antagonist action versus glucagon at the GLP-1R

Ex(9–39) is a GLP-1R antagonist and it binds to the GLP-1R ECD despite lacking the N-terminal domain of agonist peptides such as GLP-1 (HAEGTFTS) and Ex-4 (HGEGTFTS) (Fig. 1). Thus, Ex(9–39) competes with, and displaces the binding of, agonists to the GLP-1R. This property of Ex(9–39) can be explained on the basis of the recently determined GLP-1R-Ex-P5 cryo-EM structure in which the peptide Ex-P5 contains the VRLFIEWLK sequence present within Ex(9–39) that confers binding to the GLP-1R ECD (42). Our structural model, based on the GLP-1R-Ex-P5 cryo-EM structure, depicts the Ex(9–39) binding elements that interact with the rat GLP-1R (Fig. 6*f*).

Site-directed receptor mutagenesis was previously used to investigate interactions of the agonist exendin-4 with the GLP-1R (38). Amino acid residues that were mutated correspond to Tyr-69, Tyr-88, Leu-89, Pro-90, and Leu-123 (Fig. 6*f*). In binding assays, the P90A and L123A mutations resulted in loss of receptor affinity for exendin-4 (38). This is significant because these same amino acids are predicted by our model to constitute a binding interface for Ex(9–39) to the GLP-1R. In contrast, Y69A, Y88A, and L89A mutations were reported to reduce GLP-1R expression (38).

When comparing the amino acid sequence of Ex(9–39) with that of GLP-1 and glucagon (Fig. 1), an important difference is the presence of Lys-19 in Ex(9–39) instead of Val-36 in GLP-1 or Met-27 in glucagon. Lys-19 may form a salt bridge with Asp-67 of the GLP-1R ECD, thereby strengthening its binding so that it acts as a strong competitive antagonist (Fig. 6*f*). Additional interactions with Tyr-69 and Leu-123 of the ECD are predicted to be conferred by Phe-14, Ile-15, Leu-18, and Lys-19 of Ex(9–39) (Fig. 6*f*). In
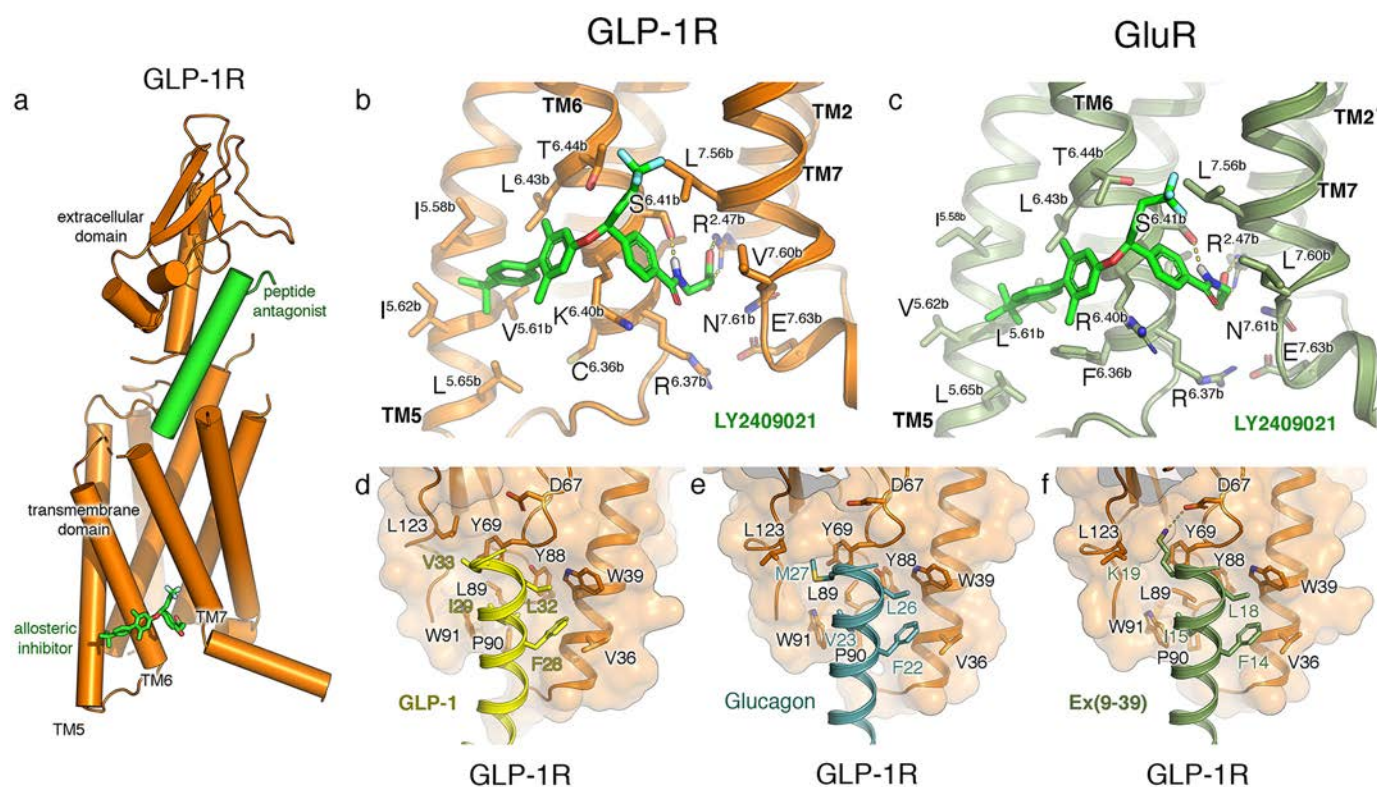
Figure 6. Docking studies for antagonist and agonist binding to the GLP-1R and GluR. *a,* predicted topology of allosteric inhibitor antagonist LY2409021 and peptide antagonist Ex(9–39) binding to the GLP-1R. *b,* putative binding modes of LY2409021 (*green stick* representation) to the rat GLP-1R (*orange cartoon* representation). Electrostatic interactions are shown in *yellow dashed lines*. *c,* binding mode of LY2409021 (*green stick* representation) docked to the rat GluR (*dark green cartoon* representation) at the transmembrane allosteric site. *Letters in superscripts* in *b* and *c* denote the TM in which the amino acid residue is located, followed by the position in that helix, where the most conserved residue has the number 50, and the *letter b* denotes GPCR family (*e.g.* 6.50b is the most conserved amino acid in TM6 for family B, the next residue in sequence is 6.51b, etc.). *d,* binding recognition of GLP-1 (*yellow*) to the rat GLP-1R ECD (*orange*) obtained from PDB code 3IOL. *e,* binding mode of glucagon N-terminal part (*blue*) to the rat GLP-1R ECD (*orange*). *f,* binding of Ex(9–39) (in *green*) to the rat GLP-1R ECD (*orange*). *Black font* in *d–f* corresponds to the rat GLP-1R residue numbering scheme (same as for the human GLP-1R). Residues within GLP-1 (*yellow*), glucagon (*blue*), and Ex(9–39) are indicated in colored font.

this regard, Asp-67 was reported to be an essential residue for peptide binding to the GLP-1R (43, 44).

des-His^1-[Glu^9]glucagon blocks glucagon action at the GluR but is without effect at the GLP-1R

Seeking a more specific GluR antagonist, we investigated the possible usefulness of GluR antagonist des-His^1-[Glu^9]glucagon (23) to differentiate between actions of glucagon that are mediated by the GluR or GLP-1R. In assays using HEK293-GluR cells, des-His^1-[Glu^9]glucagon fully suppressed the agonist action of glucagon (Fig. 7, a_1–a_3). Complete block was measured at 3.0 μM, and the IC$_{50}$ value was 0.2 μM. However, for HEK293-GLP-1R cells, des-His^1-[Glu^9]glucagon did not significantly alter the agonist actions of GLP-1 or glucagon, although a small inhibitory trend was noted at high concentrations of the antagonist (Fig. 7, b_1–b_3 and c_1–c_3). Thus, compared with LY2409021 and MK 0893, the antagonist action of des-His^1-[Glu^9]glucagon was highly selective for the GluR.

Glucagon dually regulates the GluR and GLP-1R in a pancreatic β-cell line

Moens *et al.* (45) originally reported that glucagon secreted from islet α-cells exerted an intra-islet paracrine hormone effect to stimulate the GluR and GLP-1R on β-cells. More recently, it was reported that under conditions of stress, α-cells

secrete GLP-1 in addition to glucagon (46–53). Thus, there is new interest to identify intra-islet actions of glucagon and GLP-1, and in this regard, it is necessary to validate the receptor specificity of commonly used GluR and GLP-1R agonists and antagonists.

Here, we used the INS-1 832/13 β-cell line as a model system with which to investigate the promiscuous nature of GPCR agonist and antagonist action, while also evaluating the relative importance of glucagon agonist action at the β-cell GluR *versus* GLP-1R. Consistent with findings obtained using HEK293 cells, LY2409021 and MK 0893 each reduced the dose-dependent actions of glucagon (Fig. 8, a_1–a_3) and GLP-1 (Fig. 8, b_1–b_3) to raise levels of cAMP in INS-1 832/13 cells. However, these antagonists had little or no effect on their own (Figs. S2c and S6f). Such findings are expected because INS-1 832/13 cells co-express the GluR and GLP-1R. However, because of their promiscuous GPCR antagonist actions, LY2409021 and MK 0893 are not suitable tools with which to define the relative importance of glucagon action at the GluR *versus* GLP-1R in β-cells.

The GLP-1R antagonist Ex(9–39) reduced but did not fully block the agonist action of glucagon to raise levels of cAMP in INS-1 832/13 cells (Fig. 8c$_1$). In contrast, Ex(9–39) fully blocked the action of GLP-1 (Fig. 8c$_2$), while having no effect on its own
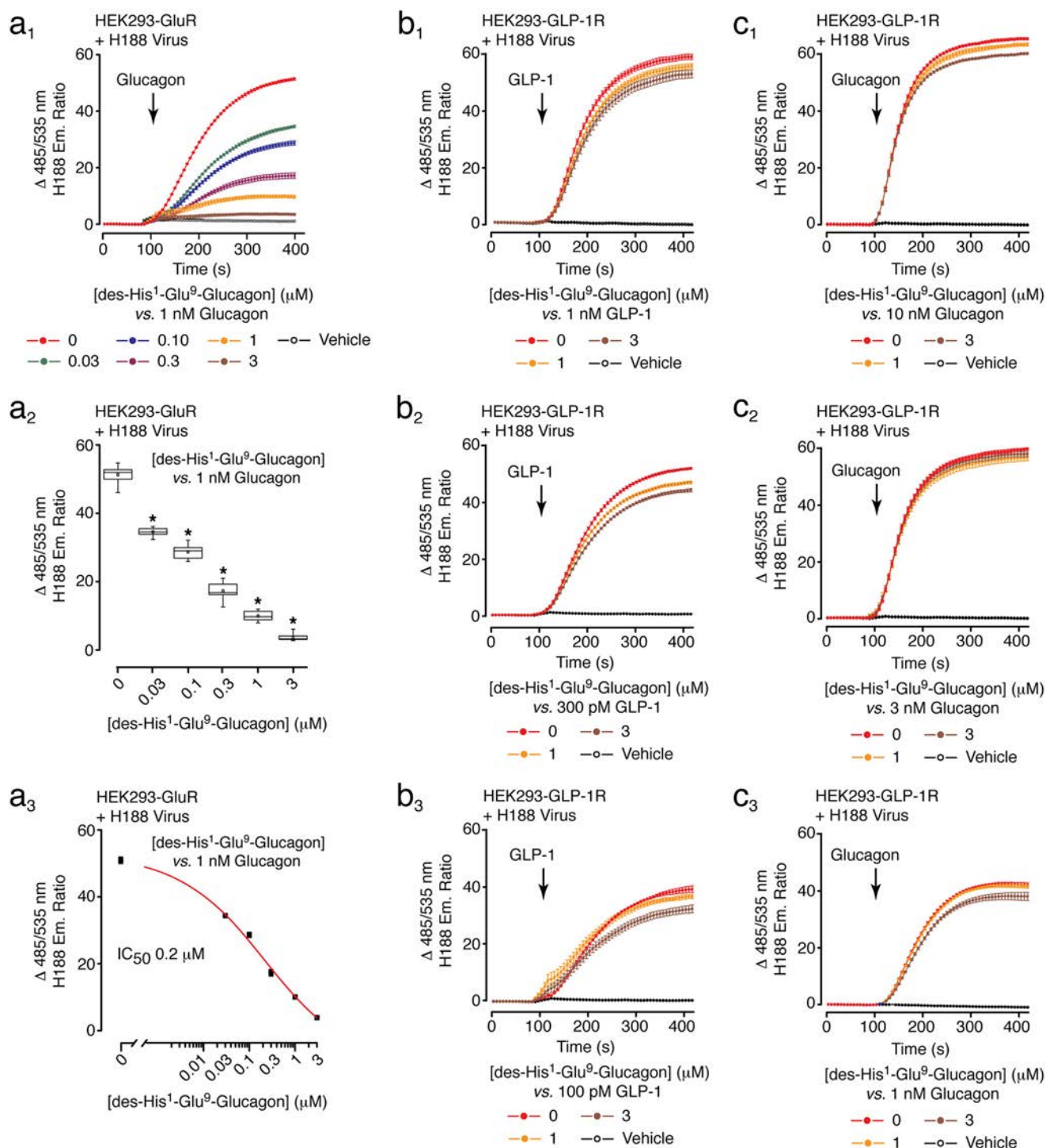
Figure 7. des-His[1][Glu[9]]glucagon is a specific GluR antagonist. a_1–a_3, FRET data (a_1), box-and-whisker plot (a_2), and dose-response plot (a_3) summarizing findings in which des-His[1]-[Glu[9]]glucagon (IC$_{50}$ 0.2 μM) blocked glucagon (1 nM) action in HEK293-GluR cells. b_1–b_3, des-His[1]-[Glu[9]]glucagon (1 or 3 μM) failed to block GLP-1 (1 nM and 300 or 100 pM) action in HEK293-GLP-1R cells. c_1–c_3, des-His[1]-[Glu[9]]glucagon (1 or 3 μM) failed to block glucagon (10, 3, or 1 nM) action in HEK293-GLP-1R cells. * indicates a p value of < 0.01, one-way ANOVA with post hoc Tukey. Comparisons in a_2 are between cells not treated (vehicle control) or treated with the indicated concentrations of des-His[1]-[Glu[9]]glucagon.

(Fig. 8c_3). These findings are expected if the action of glucagon is dually mediated by the GluR and the GLP-1R, whereas the action of GLP-1 is mediated solely by the GLP-1R. The key to interpretation of these findings is the fact that Ex(9–39) failed to alter the agonist action of glucagon at the GluR in HEK293-GluR cells (Fig. S7d). However, Ex(9–39) did block GLP-1 and glucagon agonist action at the GLP-1R in HEK293-GLP-1R

cells (Fig. 5, $a_{1–3}$ and $c_{1–3}$). Thus, for INS-1 832/13 cells, we interpret the Ex(9–39)-insensitive agonist action of glucagon to be mediated by the GluR, whereas glucagon acts at the GLP-1R in an Ex(9–39)-sensitive manner.

A dual agonist action of glucagon at the β-cell GluR and GLP-1R is further supported by studies using INS-1 832/13 cells treated with the GluR antagonist des-His[1]-[Glu[9]]glucagon. These studies
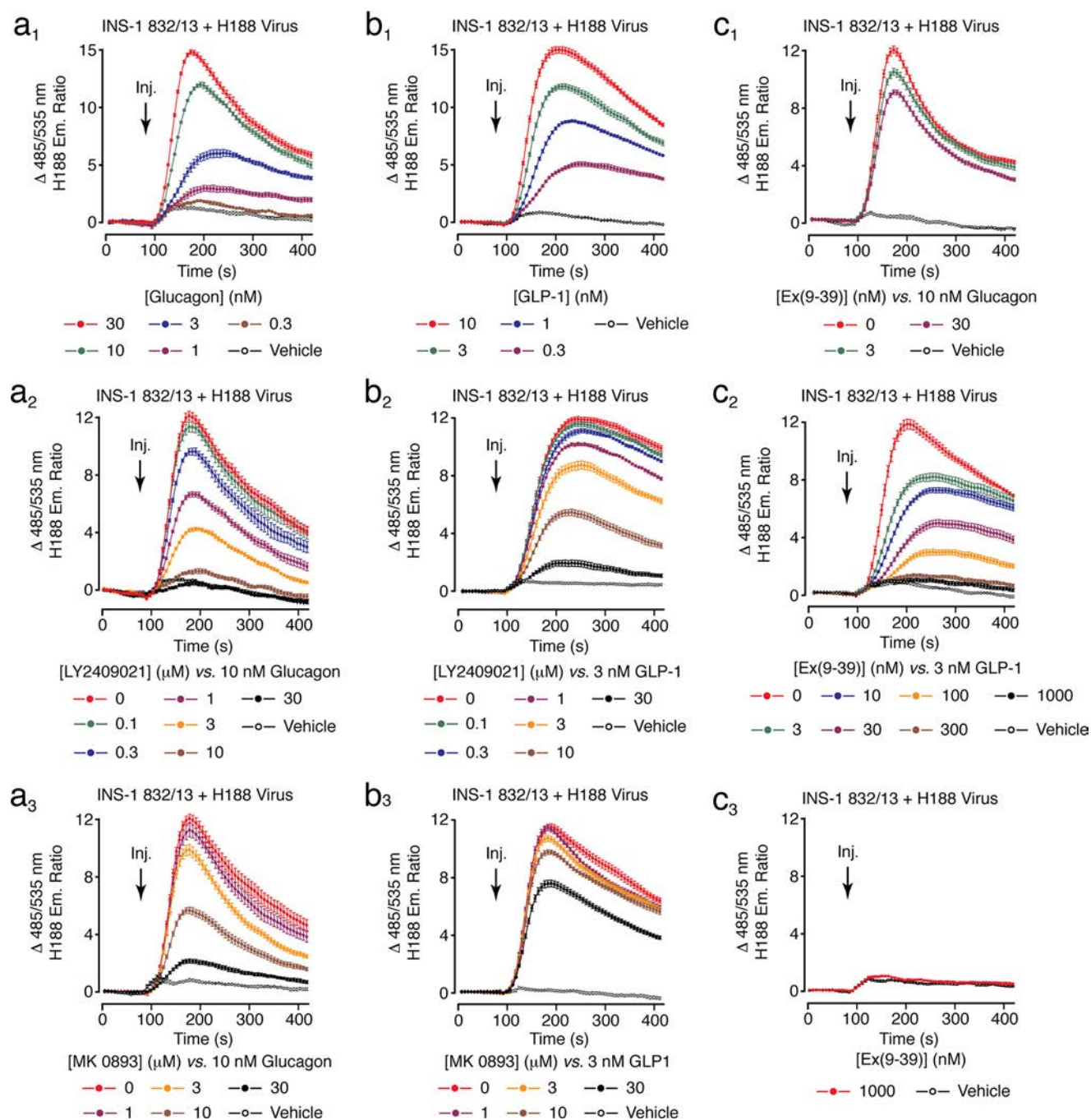
Figure 8. LY2409021, MK 0893, and Ex(9–39) antagonist actions in INS-1 832/13 cells. a_1–a_3, dose-dependent action of glucagon (a_1) was inhibited by LY2409021 (a_2) and MK 0893 (a_3). b_1–b_3, dose-dependent action of GLP-1 (b_1) was inhibited by LY2409021 (b_2) and MK 0893 (b_3). c_1–c_3, Ex(9–39) (3 or 30 nM) reduced but did not block the action of 10 nM glucagon (c_1), whereas it fully inhibited the action of 3 nM GLP-1 (c_2), while having no effect on its own when tested at 1000 nM (c_3).

revealed that des-His[1]-[Glu[9]]glucagon reduced but did not fully block the agonist action of glucagon (Fig. 9*a*). In contrast, it failed to alter the agonist action of GLP-1 (Fig. 9*b*), nor did it exert any effect on its own (Fig. 9*c*). Such outcomes are interpretable based on findings obtained using HEK293 cells in which it was established that des-His[1]-[Glu[9]]glucagon acted as a specific GluR antagonist with no detectable action at the GLP-1R (Fig. 7). Thus, for INS-1 832/13 cells, treatment with des-His[1]-[Glu[9]]glucagon revealed a residual agonist action of glucagon that was most likely mediated by the GLP-1R (Fig. 9*a*).

Findings summarized above for INS-1 832/13 cells led us to predict that the des-His[1]-[Glu[9]]glucagon-insensitive action of glucagon should be eliminated by the GLP-1R-specific antagonist Ex(9–39). To test this prediction, INS-1 832/13 cells were treated with des-His[1]-[Glu[9]]glucagon in the absence or presence of Ex(9–39). Simultaneously, the agonist action of glucagon was monitored. For cells treated only with des-His[1]-[Glu[9]]glucagon, there existed a residual-stimulatory action of glucagon mediated by the GLP-1R, and this residual action of glucagon was nearly eliminated when cells were co-treated with

GPCR agonist and antagonist actions

des-His[1]-[Glu[9]]glucagon and Ex(9–39) (Fig. 9d). An additional example from an identical replicate experiment is provided in which the relative contributions of the GluR and GLP-1R to glucagon agonist action are illustrated (Fig. 9e). In summary,

this analysis using specific GluR and GLP-1R antagonists indicated that the Ex(9–39)-sensitive component of glucagon agonist action in INS-1 832/13 cells resulted from the stimulatory action of glucagon at the GLP-1R.
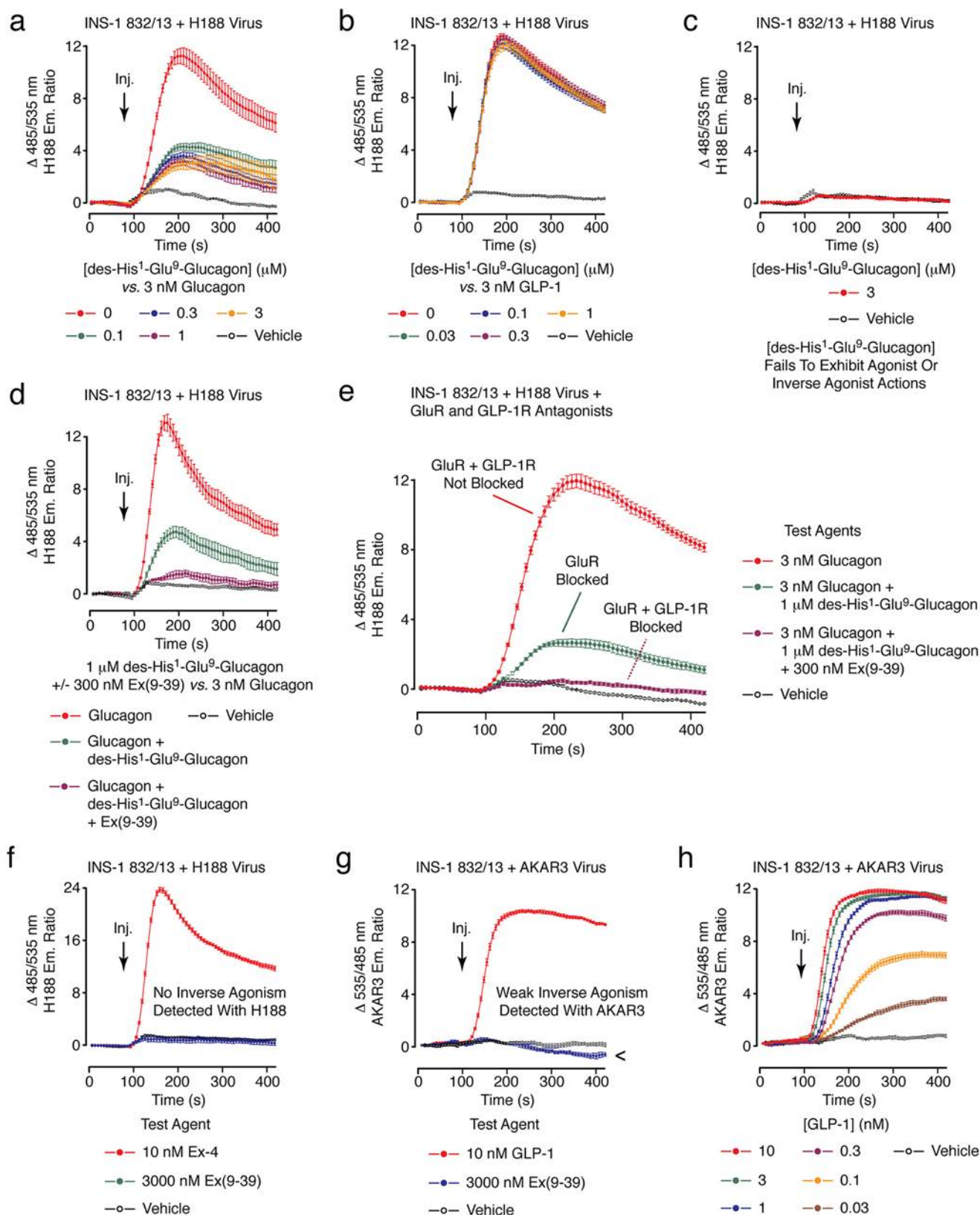
Finally, we investigated a potential inverse agonist action of Ex(9–39) originally reported for a mouse β-cell line (54). Inverse agonism should be detectable as a decrease of the H188 FRET ratio that signifies reduced levels of cAMP, yet no such ΔFRET was measured in response to Ex(9–39) using HEK293-GLP-1R cells (Fig. S7f). Studies with INS-1 832/13 cells transduced with H188 also provided no evidence for inverse agonism (Fig. 9f). However, weak inverse agonism was measured using an AKAR3 FRET reporter that is highly sensitive to cAMP signaling in this assay (55) and that responds to GLP-1 (Fig. 9, *g* and *h*).

GGP817 is an NPY2R agonist that reduces levels of cAMP

Because GGP817 contains a C-terminal fragment of PYY(3–36) fused to glucagon, we sought to determine whether it might bind to NPY2R to activate G_i proteins, thereby reducing levels of cAMP. To test this, HEK293-H188-C24 cells were transfected with human NPY2R (56) so that cAMP-lowering actions of GGP817 and NPY2R agonist PYY(3–36) could be compared. In view of the fact that HEK293-H188-C24 cells have low basal adenylyl cyclase activity and low basal levels of cAMP (27), we used adenosine (acting at endogenous A_{2B} receptors) or forskolin (acting at adenylyl cyclase) to initially enhance cyclase activity, thereby raising levels of cAMP prior to inhibitory agonist treatment. In this manner, an NPY2R-mediated counterregulatory action of GGP817 to lower levels of cAMP was evaluated.

When HEK293-H188-C24 cells expressing NPY2R were stimulated with adenosine (2 μM), levels of cAMP rose, and this effect was counteracted by GGP817 (10–1,000 nM) (Fig. 10, a_1–a_3). By comparing cells not treated or treated with NPY2R antagonist BIIE0246 (500 nM), it was established that the cAMP-lowering action of GGP817 was NPY2R-mediated (*cf.* Fig. 10, b_1 and b_2). Importantly, GGP817 was without effect in HEK293-H188-C24 cells transfected with an empty vector (EV) that served as a negative control (Fig. 10b_3). NPY2R agonist PYY(3–36) replicated the cAMP-lowering action of GGP817 across similar dose ranges (Fig. 10, c_1–c_3). In fact, the IC_{50} values for GGP817 (19 nM) and PYY(3–36) (18 nM) agonist actions were nearly identical (*cf.* Fig. 10, a_3 and c_3). To obtain independent confirmation of these findings using adenosine, we demonstrated that GGP817 counteracted the cAMP-elevating action of forskolin in assays using HEK293-H188-C24 cells transfected with NPY2R but not the EV (Fig. 10, d_1 and d_2). Finally, we demonstrated that in an assay using forskolin instead of adenosine, the cAMP-lowering action of GGP817 was reproduced by PYY(3–36) (Fig. 10d_3).

Discussion

FRET assays reveal novel features of family B GPCR agonist and antagonist action

The primary goal of this study was to apply new high-throughput FRET assay technology to real-time analysis of GPCR agonist and antagonist action in living cells so that a determination could be made concerning the specificity with which GluR and GLP-1R agonists and antagonists act to control intracellular levels of cAMP. To test for physiological significance, this analysis included not only an assessment of agonist or antagonist action at recombinant GPCRs expressed in HEK293 cells, but also endogenous GPCRs expressed in INS-1 832/13 cells.

These approaches revealed that the GluR antagonists LY2409021 and MK 0893 exerted significant off-target effects to block agonist action at the GLP-1R and GIP-R. This analysis also demonstrated that des-His[1]-[Glu[9]]glucagon is a specific GluR antagonist in that it lacks any capacity to block glucagon or GLP-1 agonist action at the GLP-1R. Furthermore, Ex(9–39) was shown to be a specific GLP-1R antagonist because it blocked the actions of glucagon and GLP-1 at the GLP-1R, whereas it failed to block the action of glucagon at the GluR. Findings reported here also established the capacity of glucagon to exert a dual agonist effect to simultaneously activate endogenous glucagon and GLP-1 receptors expressed in INS-1 832/13 cells.

We also report that the hybrid peptide GGP817 acted as a triagonist at the GluR, GLP-1R, and NPYR2. These findings are understandable because GGP817 contains full-length glucagon fused at its C terminus to a 12-amino acid C-terminal fragment of PPY. Triagonist properties of GGP817 were validated in assays that monitored its GluR- and GLP-R–mediated actions to raise levels of cAMP, or in assays that monitored its NPY2R-mediated action to lower levels of cAMP. Such findings establish GGP817 to be a prototype triagonist peptide with biological actions that are of potential medical relevance to the treatment of T2D and obesity.

Pharmacological properties of GluR, GLP-1R, and NPY2R agonists and antagonists

In FRET assays conducted in a 96-well format using the biosensor H188, the agonist action of glucagon at the GluR was monitored in real time over a time span of 0–400 s. As expected, this action of glucagon was inhibited by the allosteric GluR inhibitors LY2409021 and MK 0893. The action of glucagon was also blocked by the orthosteric GluR antagonist des-His[1]-[Glu[9]]glucagon, but not by the orthosteric GLP-1R antagonist Ex(9–39). Neither GLP-1 nor Ex-4 exerted stimulatory effects at the GluR. However, GGP817 was a full agonist (EC_{50} 183 nM) at the GluR, as judged by the maximal ΔFRET moni-

Figure 9. Dual regulation of the GluR and GLP-1R by glucagon in INS-1 832/13 cells. *a,* des-His[1]-[Glu[9]]glucagon (0.1–3 μM) reduced but did not block the action of glucagon (3 nM). *b,* the action of GLP-1 (3 nM) was unaffected by des-His[1]-[Glu[9]]glucagon (0.1–3 μM). *c,* des-His[1]-[Glu[9]]glucagon (3 μM) failed to exert any agonist or inverse agonist effect. *d* and *e,* the action of glucagon (3 nM) was fully suppressed during combined administration of des-His[1]-[Glu[9]]glucagon (1 μM) and Ex(9–39) (300 nM). *f,* no inverse agonist action of Ex(9–39) (3,000 nM) to lower levels of cAMP was measurable for INS-1 832/13 cells transduced with the FRET reporter H188 that has less affinity for cAMP compared with PKA regulatory subunits. *g,* Ex(9–39) exerted a weak inverse agonist effect to lower levels of cAMP for INS-1 832/13 cells transduced with the FRET reporter AKAR3 that is a substrate for PKA-mediated phosphorylation, and that indirectly monitors binding of cAMP to its high-affinity receptor on PKA. *h,* AKAR3 expressed in INS-1 832/13 cells reported GLP-1-stimulated cAMP production, but the dynamic range of AKAR3 was limited compared with H188. Note that when levels of cAMP rise, H188 reports a decrease of FRET that is displayed here as the Δ485/538 ratio, whereas AKAR3 reports an increase of FRET displayed here as the Δ535/485 ratio.
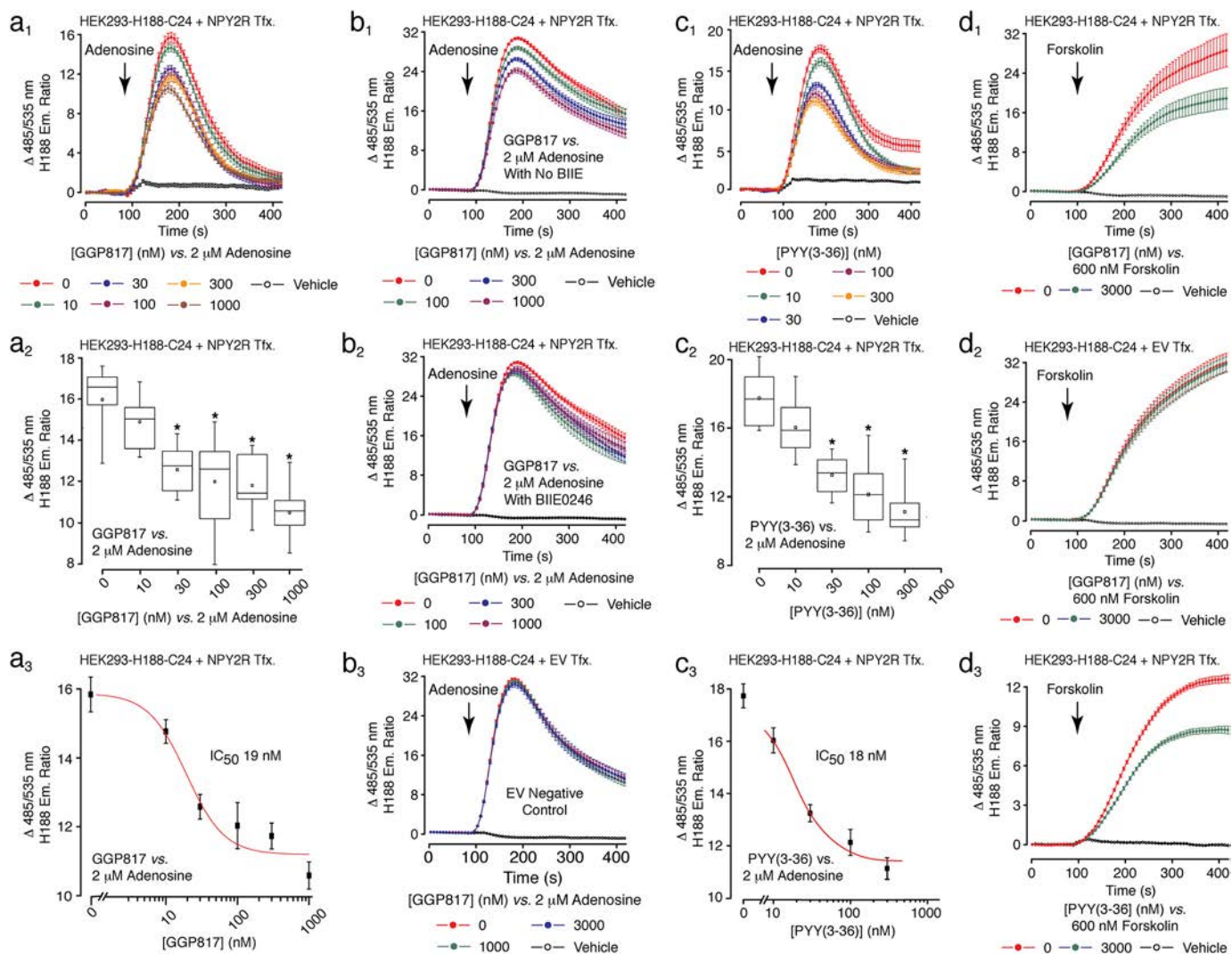
Figure 10. GGP817 and PYY(3–36) signal via NPY2R to inhibit cAMP production. a_1–a_3, FRET data (a_1), box-and-whisker plot (a_2), and dose-response plot (a_3) summarizing findings in which GGP817 (IC$_{50}$ 19 nM) counteracted the cAMP-elevating action of adenosine (2 μM) in HEK293-H188-C24 cells transfected with NPY2R. b_1 and b_2, comparisons of findings obtained using HEK293-H188-C24 cells not treated (b_1) or treated (b_2) with NPY2R antagonist BIIE0246 (2 μM). Note that BIIE0246 blocked the cAMP-lowering action of GGP817 under conditions in which cells were also treated with adenosine (2 μM). b_3, negative control demonstrating that GGP817 was without effect in HEK293-H188-C24 cells transfected with the empty vector (*EV*) and treated with adenosine. c_1–c_3, FRET data (a_1), box-and-whisker plot (a_2), and dose-response plot (a_3) summarizing findings in which PYY(3–36) (IC$_{50}$ 18 nM) counteracted the cAMP-elevating action of adenosine (2 μM) in HEK293-H188-C24 cells transfected with NPY2R. d_1 and d_2, GGP817 reduced levels of cAMP in HEK293-H188-C24 transfected with NPY2R and treated with forskolin (d_1), whereas it was without effect in cells transfected with the EV (d_2). d_3, a cAMP-lowering action of PYY(3–36) was also measured in HEK293-H188-C24 transfected with NPY2R and treated with forskolin. For a_2 and c_2, the * indicates a p value of < 0.01, one-way ANOVA with post hoc Tukey when comparing the action of adenosine in cells not treated (vehicle control) or treated with the indicated concentrations of GGP817 or PYY(3–36).

tored in this assay. This agonist action of GGP817 at the GluR was blocked by LY2409021 but not by Ex(9–39).

A nonconventional agonist action of glucagon to stimulate the GLP-1R was also measured when testing high concentrations of glucagon. However, the EC$_{50}$ value for glucagon action at the GLP-1R was 4.9 nM, whereas that of GLP-1 was 65 pM. Still, high concentrations of glucagon did produce a full agonist effect. This action of glucagon at the GLP1-R was blocked by LY2409021, MK 0893, and Ex(9–39), whereas des-His^1-[Glu^9]glucagon was without effect. Further analysis revealed that Ex-4 (EC$_{50}$ 30 pM) and GGP817 (EC$_{50}$ 61 nM) exerted full agonist actions at the GLP-1R, and that these effects were also inhibited by LY2409021, MK 0893, and Ex(9–39). Evidence for an inverse agonist action of Ex(9–39) was obtained only in studies of INS-1 832/13 cells transduced with AKAR3.

GGP817 exhibited triagonist properties so that it acted at the GluR (EC$_{50}$ 183 nM), GLP-1R (EC$_{50}$ 61 nM), and NPY2R (IC$_{50}$ 19 nM). Thus, GGP817 reproduced the natural inhibitory action of NPY2R agonist PYY(3–36) (IC$_{50}$ 18 nM) in this FRET assay using HEK293 cells transfected with NPY2R. Previously, we reported the properties of EP45, a dual agonist composed of Ex-4 and PYY, which in contrast acts as an agonist only at the GLP-1R and NPY2R (27).

Dual GluR- and GLP-1R–mediated actions of glucagon in INS-1 832/13 cells

Our interest in the pharmacology of family B GPCRs was prompted by a new appreciation that glucagon and GLP-1 act as paracrine hormones within the islets of Langerhans to stimulate glucagon and GLP-1 receptors located on islet β-cells.

Normally, glucagon is secreted from islet α-cells that are adjacent to these β-cells. However, under conditions of stress, as occurs in T2D, α-cells undergo a phenotypic switch so that they are able to synthesize and secrete GLP-1 in addition to glucagon (46–53). Thus, local intra-islet paracrine actions of glucagon and GLP-1 may serve as important determinants of β-cell function, and in fact, one recent study using glucagon and GLP-1 receptor knockout mice supports this concept (52).

Studies reported here indicate that high concentrations of glucagon released from α-cells might act within the volume-restricted microenvironment of the islet to stimulate the β-cell GLP-1R despite a substantially lower affinity of glucagon for the GLP-1R. Superimposed on this nonconventional action of glucagon is its conventional action to activate the GluR expressed on β-cells (45, 53). These actions of glucagon are likely to be complemented by the action of intra-islet GLP-1 released from α-cells to stimulate the β-cell GLP-1R (52). The net effect is that glucagon and GLP-1 coordinately stimulate cAMP production so that β-cell functionality is enhanced in the healthy state or "repaired" under conditions of T2D (57–62).

New findings using the INS-1 832/13 β-cell line are summarized as follows: 1) glucagon is a dual β-cell GluR and GLP-1R agonist when tested at high concentrations that may exist in islets; 2) LY2409021 and MK 0893 are promiscuous antagonists at the β-cell GluR and GLP-1R; 3) Ex(9−39) is a specific GLP1-R antagonist, but this effect is not restricted to antagonism of GLP-1 action because it also blocks glucagon action at the GLP-1R; and 4) des-His^1-[Gluc^9]glucagon is a specific GluR antagonist.

It is important to note that interpretation of prior *in vivo* studies using systemically administered GluR and GLP-1R antagonists are clouded by uncertainties concerning the specificity with which these antagonists target the GluR or GLP-1R. LY2409021 is considered to be a selective GluR antagonist *in vivo* (22, 63, 64), whereas Ex(9−39) is considered to be a selective GLP-1R antagonist *in vivo* (65–68). However, we find that LY2409021 acts with similar IC$_{50}$ values as an antagonist of glucagon, GLP-1, and GIP action at the GluR, GLP-1R, and GIP-R. Furthermore, we find that Ex(9−39) acts not simply to block GLP-1 action at the GLP-1R but also glucagon action at the GLP-1R.

Computational modeling predicts conserved features of ligand binding to the GluR and GLP-1R

As is the case for all GPCRs, the GLP-1R consists of an extracellular N-terminal domain (N-domain), an intracellular C-terminal region, and seven TMs that are connected to each other by three extracellular loops (ELs) and also three intracellular loops (10, 69). The ELs and TMs form the J-domain of receptor that binds GLP-1. GLP-1 interacts with the GLP-1R according to a two-step model. In the first step, the C-terminal region of GLP-1 interacts with the receptor's N-domain, thereby providing an "affinity-trap" that facilitates a second step in which the N-terminal region of GLP-1 binds to the J-domain so that the receptor is activated. Although exendin(9−39) contains a C terminus that allows its selective binding to the N-domain, it is unable to interact with the J-domain, thereby explaining its ability to act as orthosteric antagonist of GLP-1R activation.

The mode of binding of the allosteric inhibitor LY2409021 to family B GPCRs is predicted here on the basis of computational receptor modeling, and it is understandable based on prior models that explain how conformational changes of the TMs located within the J-domain allow functional interactions of family B receptors with their downstream G proteins. Allosteric inhibitors of GPCR signaling reduce agonist binding and receptor activation by intercalating between the TMs or by binding outside the TMs. The latter mechanism is suggested from the crystal structure complex formed between the GluR and its allosteric antagonist MK 0893 that is structurally related to LY2409021 (26). It is also suggested by crystal structure complexes formed between the GLP1-R and its allosteric antagonists NNC0640 and PF-06372222 (36). Specifically, these allosteric inhibitors interact with a structurally conserved binding pocket located outside TM5, TM6, and TM7 of the receptor, thus restricting the outward helical movement of TM6, which is essential for receptor activation and G protein coupling.

Because we found that LY2409021 blocked glucagon action at both the GluR and the GLP-1R, while also blocking GLP-1 action at the GLP-1R, and even GIP action at the GIP-R, we propose that LY2409021 recapitulates the allosteric inhibitor action of MK 0893 by interacting with the conserved binding pocket that is present within each of these receptors and that is located outside TM5, TM6, and TM7 (Fig. 6). Such findings are of potential clinical relevance in view of the fact that they may explain a promiscuous antagonist action of LY2409021, and other allosteric inhibitors related in structure to it, at multiple GPCRs, rather than exerting pure GluR selectivity. To what extent these allosteric inhibitors have any therapeutic value remains to be determined. Weight gain, increased blood pressure, and hepatic abnormalities were reported for patients administered LY2409021 and MK 0893 (63, 70), and both compounds have been withdrawn from clinical trials.

It is also notable that Ex(9−39) acted not simply as an antagonist of GLP-1 action at the GLP-1R, but also as an antagonist of glucagon action at the GLP-1R. These *in vitro* findings are important to the interpretation of prior *in vivo* studies in which stimulatory actions of glucagon at the GLP-1R were not seriously considered. It seems that systemically administered Ex(9−39) might block glucagon agonist action at the GLP-1R, not only in the islets, but also in other tissues that express the GLP-1R. This nonconventional action of Ex(9−39) might be explained by its ability to competitively inhibit binding of glucagon to the extracellularly-oriented N-domain of the GLP-1R where a structurally conserved binding motif determines the selectivity of ligand–receptor interactions (Fig. 6).

Triagonist properties of GGP817 acting at the GluR, GLP-1R, and NPY2R

When considering the herein reported triagonist properties of hybrid peptide GGP817, it can be concluded that this peptide's glucagon amino acid sequence motif mediates agonist actions at the GluR and GLP-1R, whereas NPY2R agonism is conferred by the peptide's C terminus that itself contains a 12-amino acid C-terminal fragment of PYY. Although GGP817 has lower affinity for the GluR and GLP-1R compared with glucagon and GLP-1, it serves as a prototype that might be of

use for future studies directed at the design of triagonists with "balanced" agonism at the GluR, GLP-1R, and NPY2R.

Because GGP817 exhibits triagonism at the GluR, GLP-1R, and NPY2R, it might exhibit desirable *in vivo* metabolic actions not previously reported for hybrid peptides (1–9). In this regard, a predicted profile of action for GGP817 would be as follows: 1) GluR agonism leading to energy expenditure and reduced fat mass; 2) GLP-1R agonism with improved β-cell insulin secretion and glucoregulation even in the context of increased hepatic glucose output because of GluR agonism; and 3) GLP-1R and NPY2R agonism leading to appetite suppression. Interestingly, it was recently reported that combined administration of Ex-4 and PYY(3–36) led to a synergistic suppression of appetite in mice (71). Thus, it will be important to determine whether a triagonist such as GGP817 emulates the synergistic co-agonist actions of Ex-4 and PYY(3–36) to suppress appetite through dual-stimulatory effects at hypothalamic NPY2R and GLP-1R. Just as important, GGP817 will still need to be profiled across other receptors before advancement as a therapeutic candidate.

Conclusion

Current efforts in drug discovery research for the treatment of obesity and diabetes include the testing of hybrid peptides with dual or triagonist actions at the NYP2R, GluR, GLP-1R, GIP-R, and other GPCRs of major relevance to metabolic homeostasis. Findings reported here emphasize the importance of validating receptor selectivities for dual or triagonists, especially with respect to potential actions of the glucagon moiety acting at the GLP-1R. Future research using pharmacological and genetic manipulation of family B GPCRs should take into account potential confounding off-target actions of conventional receptor antagonists, as reported here for inhibitory effects of LY2409021 at the GLP-1R.

Experimental procedures

Cell culture

The parental HEK293 cell line was obtained from the American Type Culture Collection (ATCC, Manassas, VA). HEK293 cells stably expressing the human GLP-1R at a density of 150,000 receptors/cell were obtained from Novo Nordisk A/S (Bagsvaerd, Denmark) (72). HEK293 cells stably expressing the rat GlucR at a density of 250,000 receptors/cell were obtained from T. P. Sakmar, A. M. Cypess, and C. G. Unson (The Rockefeller University) (73, 74). HEK293 cells stably expressing the rat GIP-R at a receptor density that has yet to be determined were obtained from T. J. Kieffer (University of British Columbia) (75). HEK293 cells stably expressing H188 were generated by O. G. Chepurny in the Holz laboratory (27). All cell cultures were maintained in Dulbecco's modified Eagle's medium containing 25 mM glucose and supplemented with 10% fetal bovine serum and 1% penicillin/streptomycin. Cell cultures equilibrated at 37 °C in a humidified incubator that was gassed with 5% CO_2 were passaged once a week. Culture media and additives were obtained from ThermoFisher Scientific (Waltham, MA).

Cell transfection

Transient transfections were performed using Lipofectamine and Plus Reagent (from ThermoFisher Scientific) using the methodol-

ogy described previously by our laboratory for HEK293 cells (76). A plasmid encoding human NPY2R (I.D. NPYR20TN00) in pcDNA3.1 was from the University of Missouri-Rolla cDNA Resource Center (Rolla, MO). HEK293 cells stably expressing H188 were obtained by G418 antibiotic resistance selection using methodology described previously (27). Adenovirus for transduction of HEK293 cells was generated by a commercial vendor (ViraQuest, North Liberty, IA) using the shuttle vector pVQAd CMV K-NpA and the H188 plasmid provided by Prof. Kees Jalink (28) or the AKAR3 plasmid provided by Prof. Jin Zhang (77).

FRET reporter assay in a 96-well format

HEK293 cells stably expressing recombinant GPCRs were plated at 80% confluence on 96-well clear-bottom assay plates (Costar 3904, Corning, NY) coated with rat tail collagen (Collaborative Biomedical Products, Bedford, MA). Cells were then transduced for 16 h with H188 virus at a density of ~60,000 cells/well under conditions in which the multiplicity of infection was equivalent to 25 viral particles per cell. The culture media were removed and replaced by 200 μl/well of a standard extracellular saline (SES) solution supplemented with 11 mM glucose and 0.1% BSA. The composition of the SES was (in mM): 138 NaCl, 5.6 KCl, 2.6 $CaCl_2$, 1.2 $MgCl_2$, 11.1 glucose, and 10 Hepes (295 mosmol, pH 7.4). Real-time kinetic assays of FRET were performed using a FlexStation 3 microplate reader equipped with excitation and emission light monochromators (Molecular Devices, Sunnyvale, CA). Excitation light was delivered at 435/9 nm (455 nm cutoff), and emitted light was detected at 485/15 nm (cyan fluorescent protein) or 535/15 nm (yellow fluorescent protein) (27, 78, 79). The emission intensities were the averages of 12 excitation flashes for each time point per well. Test solutions dissolved in SES were placed in V-bottom 96-well plates (Greiner Bio-One, Monroe, NC), and an automated pipetting procedure was used to transfer 50 μl of each test solution to each well of the assay plate containing monolayers of these cells. The 485/535 emission ratio was calculated for each well, and the mean $\pm$ S.D. values for 12 wells were averaged. These FRET ratio values were normalized using baseline subtraction so that a y axis value of 0 corresponds to the initial baseline FRET ratio, whereas a value of 100 corresponds to a 100% increase (*i.e.* doubling) of the FRET ratio. The time course of the ΔFRET ratio was plotted after exporting data to Origin 8.0 (OriginLab, Northampton, MA). Origin 8.0 was also used for nonlinear regression analysis to quantify dose-response relationships.

Statistical analyses

Raw FRET data from individual experiments are expressed as the mean $\pm$ S.D. and are derived from $n = 12$ wells for each concentration of test agent. Box and whisker plots derived from these raw data show the following: mean (solid square), 25–75% range (open box), median (line across open box), minimum and maximum values (whiskers). The repeatability of findings was confirmed by performing each experiment a minimum of three times. FRET ratio data were evaluated for statistical significance by a one-way ANOVA test with a post hoc Tukey HSD test. Comparisons of individual data sets are defined in the accompanying figure legends. A p value of < 0.05 was considered to be statistically significant.

Sources of reagents

GGP817 was produced by Genscript (Piscataway, NJ) at ≥97% purity and with C-terminal amidation. Purity and identity were confirmed in-house by reversed-phase HPLC and electron spray MS, respectively. GLP-1, glucagon, Ex-4, Ex(9–39), GIP, PYY(3–36), des-His^1-[Glu^9]glucagon, GS 6201, and forskolin were from Sigma. LY2409021 and MK 0893 were from MedChemExpress (Monmouth Junction, NJ). BIIE0246 was from Tocris Biosciences (Minneapolis, MN).

Computational studies

Homology models of the receptors used in this study were made with Modeler 9.19. The rat GLP-1R and GluR sequences were obtained from Uniport (IDs P32301 and P30082, respectively) and aligned to the crystal structure sequences of the GLP-1R (PDB code 5VEW) (36) and GluR (PDB code 5EE7) (26), respectively. Structural models of the rat GLP-1R bound to GLP-1, glucagon, and Ex(9–39) were made using as a template the GLP-1R ECD-GLP-1 crystal structure (PDB code 3IOL) (38) in the first case, and the full-length GLP-1R-exendin-P5 cryo-EM structure (PDB code 6B3J) (42) for the latter two, using the rat GLP-1R sequence (Uniport ID P32301). The conserved S1.50b in TM1, H2.50b in TM2, E3.50b in TM3, W4.50b in TM4, N5.50b in TM5, G6.50b in TM6, and G7.50b in TM7 were used as reference points in all the sequence alignments. Superscripts denote the single most conserved residue among family B GPCRs, which is designated as X.50b according to the Wootten numbering scheme (37). The overall stereochemical quality of the homology models was evaluated by the discrete optimized energy and visual inspection. For evaluation of LY2409021 and MK 0893 binding to GPCRs, ligands were docked in the extracellular allosteric binding site of the receptor using VinaSH (80), a version of AutoDock Vina (81), which also takes into account sulfur and halogen bonding. The AutoDock-Tools program was used to prepare the corresponding PDBQT-protein file for the docking. The receptor was considered rigid during the docking process, although the ligand was allowed to be flexible. Docking calculations in both cases were performed using a grid box with dimensions of 26 × 26 × 26 Å, located around the binding site of MK-0893 (PDB code 5EE7) and a search space of 20 binding modes, and the search parameter was set to 5. The best docking pose was chosen on the basis of the lowest energy docking score.

Data availability

The data that support the findings of this study are available from the corresponding authors upon reasonable request.

References

1. Day, J. W., Ottaway, N., Patterson, J. T., Gelfanov, V., Smiley, D., Gidda, J., Findeisen, H., Bruemmer, D., Drucker, D. J., Chaudhary, N., Holland, J., Hembree, J., Abplanalp, W., Grant, E., Ruehl, J., *et al.* (2009) A new glucagon and GLP-1 co-agonist eliminates obesity in rodents. *Nat. Chem. Biol.* **5,** 749–757 CrossRef Medline

2. Gault, V. A., Bhat, V. K., Irwin, N., and Flatt, P. R. (2013) A novel glucagon-like peptide-1 (GLP-1)/glucagon hybrid peptide with triple-acting agonist activity at glucose-dependent insulinotropic polypeptide, GLP-1, and glucagon receptors and therapeutic potential in high fat-fed mice. *J. Biol. Chem.* **288,** 35581–35591 CrossRef Medline

3. Finan, B., Yang, B., Ottaway, N., Smiley, D. L., Ma, T., Clemmensen, C., Chabenne, J., Zhang, L., Habegger, K. M., Fischer, K., Campbell, J. E., Sandoval, D., Seeley, R. J., Bleicher, K., Uhles, S., *et al.* (2015) A rationally designed monomeric peptide triagonist corrects obesity and diabetes in rodents. *Nat. Med.* **21,** 27–36 CrossRef Medline

4. Skow, M. A., Bergmann, N. C., and Knop, F. K. (2016) Diabetes and obesity treatment based on dual incretin receptor activation: 'twincretins'. *Diabetes Obes. Metab.* **18,** 847–854 CrossRef Medline

5. Evers, A., Haack, T., Lorenz, M., Bossart, M., Elvert, R., Henkel, B., Stengelin, S., Kurz, M., Glien, M., Dudda, A., Lorenz, K., Kadereit, D., and Wagner, M. (2017) Design of novel exendin-based dual glucagon-like peptide 1 (GLP-1)/glucagon receptor agonists. *J. Med. Chem.* **60,** 4293–4303 CrossRef Medline

6. Brandt, S. J., Götz, A., Tschöp, M. H., and Müller, T. D. (2018) Gut hormone polyagonists for the treatment of type 2 diabetes. *Peptides* **100,** 190–201 CrossRef Medline

7. Sánchez-Garrido, M. A., Brandt, S. J., Clemmensen, C., Müller, T. D., DiMarchi, R. D., and Tschöp, M. H. (2017) GLP-1/glucagon receptor co-agonism for treatment of obesity. *Diabetologia* **60,** 1851–1861 CrossRef Medline

8. Müller, T. D., Finan, B., Clemmensen, C., DiMarchi, R. D., and Tschöp, M. H. (2017) The new biology and pharmacology of glucagon. *Physiol. Rev.* **97,** 721–766 CrossRef Medline

9. Capozzi, M. E., DiMarchi, R. D., Tschöp, M. H., Finan, B., and Campbell, J. E. (2018) Targeting the incretin/glucagon system with triagonists to treat diabetes. *Endocr. Rev.* **39,** 719–738 CrossRef Medline

10. Liapakis, G., Matsoukas, M. T., Karageorgos, V., Venihaki, M., and Mavromoustakos, T. (2017) Family B G protein-coupled receptors and their ligands: from structure to function. *Curr. Med. Chem.* **24,** 3323–3355 Medline

11. Parker, S. L., and Balasubramaniam, A. (2008) Neuropeptide Y Y2 receptor in health and disease. *Br. J. Pharmacol.* **153,** 420–431 CrossRef Medline

12. Scott, R. V., and Bloom, S. R. (2018) Problem or solution: the strange story of glucagon. *Peptides* **100,** 36–41 CrossRef Medline

13. Holz, G. G., and Chepurny, O. G. (2003) Glucagon-like peptide-1 synthetic analogs: new therapeutic agents for use in the treatment of diabetes mellitus. *Curr. Med. Chem.* **10,** 2471–2483 CrossRef Medline

14. Nadkarni, P., Chepurny, O. G., and Holz, G. G. (2014) Regulation of glucose homeostasis by GLP-1. *Prog. Mol. Biol. Transl. Sci.* **121,** 23–65 CrossRef Medline

15. Habib, A. M., Richards, P., Rogers, G. J., Reimann, F., and Gribble, F. M. (2013) Co-localisation and secretion of glucagon-like peptide 1 and peptide YY from primary cultured human L cells. *Diabetologia* **56,** 1413–1416 CrossRef Medline

16. Batterham, R. L., Cowley, M. A., Small, C. J., Herzog, H., Cohen, M. A., Dakin, C. L., Wren, A. M., Brynes, A. E., Low, M. J., Ghatei, M. A., Cone, R. D., and Bloom, S. R. (2002) Gut hormone PYY(3–36) physiologically inhibits food intake. *Nature* **418,** 650–654 CrossRef Medline

17. Wren, A. M., and Bloom, S. R. (2007) Gut hormones and appetite control. *Gastroenterology* **132,** 2116–2130 CrossRef Medline

18. Larsen, P. J., Tang-Christensen, M., Holst, J. J., and Orskov, C. (1997) Distribution of glucagon-like peptide-1 and other preproglucagon-derived peptides in the rat hypothalamus and brainstem. *Neuroscience* **77,** 257–270 CrossRef Medline

ASBMB

19. Alhadeff, A. L., Rupprecht, L. E., and Hayes, M. R. (2012) GLP-1 neurons in the nucleus of the solitary tract project directly to the ventral tegmental area and nucleus accumbens to control for food intake. *Endocrinology* **153**, 647–658 CrossRef Medline

20. Göke, R., Fehmann, H. C., Linn, T., Schmidt, H., Krause, M., Eng, J., and Göke, B. (1993) Exendin-4 is a high potency agonist and truncated exendin-(9–39)-amide an antagonist at the glucagon-like peptide 1-(7–36)-amide receptor of insulin-secreting beta-cells. *J. Biol. Chem.* **268**, 19650–19655 Medline

21. Thorens, B., Porret, A., Bühler, L., Deng, S. P., Morel, P., and Widmann, C. (1993) Cloning and functional expression of the human islet GLP-1 receptor. Demonstration that exendin-4 is an agonist and exendin-(9–39) an antagonist of the receptor. *Diabetes* **42**, 1678–1682 CrossRef Medline

22. Runge, S., Thøgersen, H., Madsen, K., Lau, J., and Rudolph, R. (2008) Crystal structure of the ligand-bound glucagon-like peptide-1 receptor extracellular domain. *J. Biol. Chem.* **283**, 11340–11347 CrossRef Medline

23. Unson, C. G., Andreu, D., Gurzenda, E. M., and Merrifield, R. B. (1987) Synthetic peptide antagonists of glucagon. *Proc. Natl. Acad. Sci. U.S.A.* **84**, 4083–4087 CrossRef Medline

24. Kazda, C. M., Ding, Y., Kelly, R. P., Garhyan, P., Shi, C., Lim, C. N., Fu, H., Watson, D. E., Lewin, A. J., Landschulz, W. H., Deeg, M. A., Moller, D. E., and Hardy, T. A. (2016) Evaluation of efficacy and safety of the glucagon receptor antagonist LY2409021 in patients with type 2 diabetes: 12- and 24-week phase 2 studies. *Diabetes Care* **39**, 1241–1249 CrossRef Medline

25. Xiong, Y., Guo, J., Candelore, M. R., Liang, R., Miller, C., Dallas-Yang, Q., Jiang, G., McCann, P. E., Qureshi, S. A., Tong, X., Xu, S. S., Shang, J., Vincent, S. H., Tota, L. M., Wright, M. J., *et al.* (2012) Discovery of a novel glucagon receptor antagonist *N*-[(4-{(1*S*)-1-[3-(3,5-dichlorophenyl)-5-(6-methoxynaphthalen-2-yl)-1*H*-pyrazol-1-yl]ethyl}phenyl)carbonyl]-*β*-alanine (MK-0893) for the treatment of type II diabetes. *J. Med. Chem.* **55**, 6137–6148 CrossRef Medline

26. Jazayeri, A., Doré, A. S., Lamb, D., Krishnamurthy, H., Southall, S. M., Baig, A. H., Bortolato, A., Koglin, M., Robertson, N. J., Errey, J. C., Andrews, S. P., Teobald, I., Brown, A. J., Cooke, R. M., Weir, M., and Marshall, F. H. (2016), Extra-helical binding site of a glucagon receptor antagonist. *Nature* **533**, 274–277 CrossRef Medline

27. Chepurny, O. G., Bonaccorso, R. L., Leech, C. A., Wöllert, T., Langford, G. M., Schwede, F., Roth, C. L., Doyle, R. P., and Holz, G. G. (2018) Chimeric peptide EP45 as a dual agonist at GLP-1 and NPY2R receptors. *Sci. Rep.* **8**, 3749 CrossRef Medline

28. Klarenbeek, J., Goedhart, J., van Batenburg, A., Groenewald, D., and Jalink, K. (2015) Fourth-generation Epac-based FRET sensors for cAMP feature exceptional brightness, photostability and dynamic range: characterization of dedicated sensors for FLIM, for ratiometry and with high affinity. *PLoS ONE* **10**, e0122513 CrossRef Medline

29. Dumont, Y., Cadieux, A., Doods, H., Pheng, L. H., Abounader, R., Hamel, E., Jacques, D., Regoli, D., and Quirion, R. (2000) BIIE0246, a potent and highly selective non-peptide neuropeptide Y Y2 receptor antagonist. *Br. J. Pharmacol.* **129**, 1075–1088 CrossRef Medline

30. Jelinek, L. J., Lok, S., Rosenberg, G. B., Smith, R. A., Grant, F. J., Biggs, S., Bensch, P. A., Kuijper, J. L., Sheppard, P. O., Sprecher, C. A., O'Hara, P. J., Foster, D., Walker, K. M., Chen, L. H. J., McKernan, P. A., and Kindsvogel, W. (1993) Expression cloning and signaling properties of the rat glucagon receptor. *Science* **259**, 1614–1616 CrossRef Medline

31. Thorens, B. (1992) Expression cloning of the pancreatic beta cell receptor for the gluco-incretin hormone glucagon-like peptide 1. *Proc. Natl. Acad. Sci. U.S.A.* **89**, 8641–8645 CrossRef Medline

32. Gremlich, S., Porret, A., Hani, E. H., Cherif, D., Vionnet, N., Froguel, P., and Thorens, B. (1995) Cloning, functional expression, and chromosomal localization of the human pancreatic islet glucose-dependent insulinotropic polypeptide receptor. *Diabetes* **44**, 1202–1208 CrossRef Medline

33. Cooper, J., Hill, S. J., and Alexander, S. P. (1997) An endogenous A2B adenosine receptor coupled to cyclic AMP generation in human embryonic kidney (HEK 293) cells. *Br. J. Pharmacol.* **122**, 546–550 CrossRef Medline

34. Hohmeier, H. E., Mulder, H., Chen, G., Henkel-Rieger, R., Prentki, M., and Newgard, C. B. (2000) Isolation of INS-1-derived cell lines with robust ATP-sensitive K$^+$ channel-dependent and -independent glucose-stimulated insulin secretion. *Diabetes* **49**, 424–430 CrossRef Medline

35. Zhang, H., Qiao, A., Yang, D., Yang, L., Dai, A., de Graff, C., Reedtz-Runge, S., Dharmarajan, V., Zhang, H., Han, G. W., Grant, T. D., Sierra, R. G., Weierstall, U., Nelson, G., Liu, W., *et al.* (2017) Structure of the full-length glucagon class B G-protein-coupled receptor. *Nature* **546**, 259–264 CrossRef Medline

36. Song, G., Yang, D., Wang, Y., de Graaf, C., Zhou, Q., Jiang, S., Liu, K., Cai, X., Dai, A., Lin, G., Liu, D., Wu, F., Wu, Y., Zhao, S., Ye, L., *et al.* (2017) Human GLP-1 receptor transmembrane domain structure in complex with allosteric modulators. *Nature* **546**, 312–315 CrossRef Medline

37. Wootten, D., Simms, J., Miller, L. J., Christopoulos, A., and Sexton, P. M. (2013) Polar transmembrane interactions drive formation of ligand-specific and signal pathway-biased family B G protein-coupled receptor conformations. *Proc. Natl. Acad. Sci. U.S.A.* **110**, 5211–5216 CrossRef Medline

38. Underwood, C. R., Garibay, P., Knudsen, L. B., Hastrup, S., Peters, G. H., Rudolph, R., and Reedtz-Runge, S. (2010) Crystal structure of glucagonlike peptide-1 in complex with the extracellular domain of the glucagonlike peptide-1 receptor. *J. Biol. Chem.* **285**, 723–730 CrossRef Medline

39. Zhang, Y., Sun, B., Feng, D., Hu, H., Chu, M., Qu, Q., Tarrasch, J. T., Li, S., Sun Kobilka, T., Kobilka, B. K., and Skiniotis, G. (2017) Cryo-EM structure of the activated GLP-1 receptor in complex with a G protein. *Nature* **546**, 248–253 CrossRef Medline

40. Zhang, H., Qiao, A., Yang, L., Van Eps, N., Frederiksen, K. S., Yang, D., Dai, A., Cai, X., Zhang, H., Yi, C., Cao, C., He, L., Yang, H., Lau, J., Ernst, O. P., *et al.* (2018) Structure of the glucagon receptor in complex with a glucagon analogue. *Nature* **553**, 106–110 CrossRef Medline

41. Chabenne, J., Chabenne, M. D., Zhao, Y., Levy, J., Smiley, D., Gelfanov, V., and Dimarchi, R. (2014) A glucagon analog chemically stabilized for immediate treatment of life-threatening hypoglycemia. *Mol. Metabol.* **3**, 293–300 CrossRef

42. Liang, Y. L., Khoshouei, M., Glukhova, A., Furness, S. G. B., Zhao, P., Clydesdale, L., Koole, C., Truong, T. T., Thal, D. M., Lei, S., Radjainia, M., Danev, R., Baumeister, W., Wang, M. W., Miller, L. J., *et al.* (2018) Phase-plate cryo-EM structure of a biased agonist-bound human GLP-1 receptor-Gs complex. *Nature* **555**, 121–125 CrossRef Medline

43. Xiao, Q., Jeng, W., and Wheeler, M. B. (2000) Characterization of glucagon-like peptide-1 receptor-binding determinants. *J. Mol. Endocrinol.* **25**, 321–335 CrossRef Medline

44. Dong, M., Gao, F., Pinon, D. I., and Miller, L. J. (2008) Insights into the structural basis of endogenous agonist activation of family B G protein-coupled receptors. *Mol. Endocrinol.* **22**, 1489–1499 CrossRef Medline

45. Moens, K., Flamez, D., Van Schravendijk, C., Ling, Z., Pipeleers, D., and Schuit, F. (1998) Dual glucagon recognition by pancreatic *β*-cells via glucagon and glucagon-like peptide-1 receptors. *Diabetes* **47**, 66–72 CrossRef Medline

46. Nie, Y., Nakashima, M., Brubaker, P. L., Li, Q. L., Perfetti, R., Jansen, E., Zambre, Y., Pipeleers, D., and Friedman, T. C. (2000) Regulation of pancreatic PC1 and PC2 associated with increased glucagon-like peptide 1 in diabetic rats. *J. Clin. Invest.* **105**, 955–965 CrossRef Medline

47. Whalley, N. M., Pritchard, L. E., Smith, D. M., and White, A. (2011) Processing of proglucagon to GLP-1 in pancreatic alpha-cells: is this a paracrine mechanism enabling GLP-1 to act on beta-cells? *J. Endocrinol.* **211**, 99–106 CrossRef Medline

48. Marchetti, P., Lupi, R., Bugliani, M., Kirkpatrick, C. L., Sebastiani, G., Grieco, F. A., Del Guerra, S., D'Aleo, V., Piro, S., Marselli, L., Boggi, U., Filipponi, F., Tinti, L., Salvini, L., Wollheim, C. B., *et al.* (2012) A local glucagon-like peptide 1 (GLP-1) system in human pancreatic islets. *Diabetologia* **55**, 3262–3272 CrossRef Medline

49. Donath, M. Y., and Burcelin, R. (2013) GLP-1 effects on islets: hormonal, neuronal, or paracrine? *Diabetes Care* **36**, Suppl. 2, S145–S148 CrossRef Medline

50. O'Malley, T. J., Fava, G. E., Zhang, Y., Fonseca, V. A., and Wu, H. (2014) Progressive change of intra-islet GLP-1 production during diabetes development. *Diabetes Metab. Res. Rev.* **30**, 661–668 CrossRef Medline

51. D'Alessio, D. (2016) Is GLP-1 a hormone: whether and when? *J. Diabetes Investig.* 7, Suppl. 1, 50–55 CrossRef Medline

ASBMB

52. Svendsen, B., Larsen, O., Gabe, M. B. N., Christiansen, C. B., Rosenkilde, M. M., Drucker, D. J., and Holst, J. J. (2018) Insulin secretion depends on intra-islet glucagon signaling. *Cell Rep.* **25,** 1127–1134.e2 CrossRef Medline

53. Kawai, K., Yokota, C., Ohashi, S., Watanabe, Y., and Yamashita, K. (1995) Evidence that glucagon stimulates insulin secretion through its own receptor in rats. *Diabetologia* **38,** 274–276 CrossRef Medline

54. Serre, V., Dolci, W., Schaerer, E., Scrocchi, L., Drucker, D., Efrat, S., and Thorens, B. (1998) Exendin-(9–39) is an inverse agonist of the murine glucagon-like peptide-1 receptor: implications for basal intracellular cyclic adenosine 3′,5′-monophosphate levels and beta-cell glucose competence. *Endocrinology* **139,** 4448–4454 CrossRef Medline

55. Holz, G. G., Leech, C. A., Roe, M. W., and Chepurny, O. G. (2015) High-throughput FRET assays for fast time-dependent detection of cAMP in pancreatic β-cells. *In Cyclic Nucleotide Signaling* (Cheng, X., ed) pp. 35–60, Taylor and Francis Group and CRC Press, Inc., Boca Raton, FL

56. Rose, P. M., Fernandes, P., Lynch, J. S., Frazier, S. T., Fisher, S. M., Kodukula, K., Kienzle, B., and Seethala, R. (1995) Cloning and functional expression of a cDNA encoding a human type 2 neuropeptide Y receptor. *J. Biol. Chem.* **270,** 22661–22664 CrossRef Medline

57. Holz, G. G., and Habener, J. F. (1992) Signal transduction crosstalk in the endocrine system: pancreatic beta-cells and the glucose competence concept. *Trends Biochem. Sci.* **17,** 388–393 CrossRef Medline

58. Holz, G. G., 4th., Kühtreiber, W. M., and Habener, J. F. (1993) Pancreatic beta-cells are rendered glucose-competent by the insulinotropic hormone glucagon-like peptide-1(7–37). *Nature* **361,** 362–365 CrossRef Medline

59. Chepurny, O. G., Hussain, M. A., and Holz, G. G. (2002) Exendin-4 as a stimulator of rat insulin I gene promoter activity via bZIP/CRE interactions sensitive to serine/threonine protein kinase inhibitor Ro 31-8220. *Endocrinology* **143,** 2303–2313 CrossRef Medline

60. Holz, G. G. (2004) New insights concerning the glucose-dependent insulin secretagogue action of glucagon-like peptide-1 in pancreatic beta-cells. *Horm. Metab. Res.* **36,** 787–794 CrossRef Medline

61. Holz, G. G., and Chepurny, O. G. (2005) Diabetes outfoxed by GLP-1? *Sci. STKE* **2005,** pe2 Medline

62. Leech, C. A., Dzhura, I., Chepurny, O. G., Kang, G., Schwede, F., Genieser, H. G., and Holz, G. G. (2011) Molecular physiology of glucagon-like peptide-1 insulin secretagogue action in pancreatic beta cells. *Prog. Biophys. Mol. Biol.* **107,** 236–247 CrossRef Medline

63. Kelly, R. P., Garhyan, P., Raddad, E., Fu, H., Lim, C. N., Prince, M. J., Pinaire, J. A., Loh, M. T., and Deeg, M. A. (2015) Short-term administration of the glucagon receptor antagonist LY2409021 lowers blood glucose in healthy people and in those with type 2 diabetes. *Diabetes Obes. Metab.* **17,** 414–422 CrossRef Medline

64. Guzman, C. B., Zhang, X. M., Liu, R., Regev, A., Shankar, S., Garhyan, P., Pillai, S. G., Kazda, C., Chalasani, N., and Hardy, T. A. (2017) Treatment with LY2409021, a glucagon receptor antagonist, increases liver fat in patients with type 2 diabetes. *Diabetes Obes. Metab.* **19,** 1521–1528 CrossRef Medline

65. Schirra, J., Sturm, K., Leicht, P., Arnold, R., Göke, B., and Katschiniski, M. (1998) Exendin(9–39)amide is an antagonist of glucagon-like peptide-1(7–36)amide in humans. *J. Clin. Invest.* **101,** 1421–1430 CrossRef Medline

66. Calabria, A. C., Li, C., Gallagher, P. R., Stanley, C. A., and De León, D. D. (2012) GLP-1 receptor antagonist exendin-(9–39) elevates fasting blood glucose levels in congenital hyperinsulinism owing to inactivating mutations in the ATP-sensitive K$^+$ channel. *Diabetes* **61,** 2585–2591 CrossRef Medline

67. Sathananthan, M., Farrugia, L. P., Miles, J. M., Piccinini, F., Dalla Man, C., Zinsmeister, A. R., Cobelli, C., Rizza, R. A., and Vella, A. (2013) Direct effects of exendin-(9,39) and GLP-1-(9–36)amide on insulin action, beta-cell function, and glucose metabolism in nondiabetic subjects. *Diabetes* **62,** 2752–2756 CrossRef Medline

68. Chambers, A. P., Sorrell, J. E., Haller, A., Roelofs, K., Hutch, C. R., Kim, K. S., Gutierrez-Aguilar, R., Li, B., Drucker, D. J., D'Alessio, D. A., Seeley, R. J., and Sandoval, D. A. (2017) The role of pancreatic preproglucagon in glucose homeostasis in mice. *Cell Metab.* **25,** 927–934.e3 CrossRef Medline

69. Karageorgos, V., Venihaki, M., Sakellaris, S., Pardalos, M., Kontakis, G., Matsoukas, M. T., Gravanis, A., Margioris, A., and Liapakis, G. (2018) Current understanding of the structure and function of family B GPCRs to design novel drugs. *Hormones (Athens)* **17,** 45–59 CrossRef Medline

70. Engel, S. S., Lei, X., Andryuk, P. J., Davies, M. J., Amatruda, J., Kaufman, K., and Goldstein, B. J. (2011) Efficacy and tolerability of MK-0893, a glucagon receptor antagonist (GRA), in patients with type 2 diabetes (T2DM). *Diabetes* **60,** A85

71. Kjaergaard, M., Salinas, C. B. G., Rehfeld, J. F., Secher, A., Raun, K., and Wulff, B. S. (2019) PYY(3–36) and exendin-4 reduce food intake and activate neuronal circuits in a synergistic manner in mice. *Neuropeptides* **73,** 89–95 CrossRef Medline

72. Gromada, J., Rorsman, P., Dissing, S., and Wulff, B. S. (1995) Stimulation of cloned human glucagon-like peptide 1 receptor expressed in HEK 293 cells induces cAMP-dependent activation of calcium-induced calcium release. *FEBS Lett.* **373,** 182–186 CrossRef Medline

73. Jiang, Y., Cypess, A. M., Muse, E. D., Wu, C. R., Unson, C. G., Merrifield, R. B., and Sakmar, T. P. (2001) Glucagon receptor activates extracellular signal-regulated protein kinase 1/2 via cAMP-dependent protein kinase. *Proc. Natl. Acad. Sci. U.S.A.* **98,** 10102–10107 CrossRef Medline

74. Cypess, A. M. (1999) *Signal Transduction by the Glucagon Receptor: Characterization of Ligand Binding, G Protein-Coupling, Second Messenger Generation, and Downstream Effector Activation.* Ph.D. thesis, The Rockefeller University

75. Kim, S. J., Choi, W. S., Han, J. S., Warnock, G., Fedida, D., and McIntosh, C. H. (2005) A novel mechanism for the suppression of a voltage-gated potassium channel by glucose-dependent insulinotropic polypeptide: protein kinase A-dependent endocytosis. *J. Biol. Chem.* **280,** 28692–28700 CrossRef Medline

76. Chepurny, O. G., and Holz, G. G. (2007) A novel cyclic adenosine monophosphate responsive luciferase reporter incorporating a nonpalindromic cyclic adenosine monophosphate response element provides optimal performance for use in G protein coupled receptor drug discovery efforts. *J. Biomol. Screen.* **12,** 740–746 CrossRef Medline

77. Allen, M. D., and Zhang, J. (2006) Subcellular dynamics of protein kinase A activity visualized by FRET-based reporters. *Biochem. Biophys. Res. Commun.* **348,** 716–721 CrossRef Medline

78. Chepurny, O. G., Leech, C. A., Kelley, G. G., Dzhura, I., Dzhura, E., Li, X., Rindler, M. J., Schwede, F., Genieser, H. G., and Holz, G. G. (2009) Enhanced Rap1 activation and insulin secretagogue properties of an acetoxymethyl ester of an Epac-selective cyclic AMP analog in rat INS-1 cells: studies with 8-pCPT-2′-O-Me-cAMP-AM. *J. Biol. Chem.* **284,** 10728–10736 CrossRef Medline

79. Schwede, F., Chepurny, O. G., Kaufholz, M., Bertinetti, D., Leech, C. A., Cabrera, O., Zhu, Y., Mei, F., Cheng, X., Manning Fox, J. E., MacDonald, P. E., Genieser, H. G., Herberg, F. W., and Holz, G. G. (2015) Rp-cAMPS prodrugs reveal the cAMP dependence of first-phase glucose-stimulated insulin secretion. *Mol. Endocrinol.* **29,** 988–1005 CrossRef Medline

80. Koebel, M. R., Cooper, A., Schmadeke, G., Jeon, S., Narayan, M., and Sirimulla, S. (2016) S⋯O and S⋯N sulfur bonding interactions in protein-ligand complexes: empirical considerations and scoring function. *J. Chem. Inf. Model.* **56,** 2298–2309 CrossRef Medline

81. Trott, O., and Olson, A. J. (2010) AutoDock Vina: improving the speed and accuracy of docking with a new scoring function, efficient optimization, and multithreading. *J. Comput. Chem.* **31,** 455–461 Medline

ASBMB

J. Biol. Chem. (2019) 294(10) 3514–3531 **3531**